

This is a repository copy of *Holocene mangrove dynamics and relative sea-level changes along the Tanzanian coast, East Africa*.

White Rose Research Online URL for this paper:  
<https://eprints.whiterose.ac.uk/136117/>

Version: Accepted Version

---

**Article:**

Punwong, Paramita, Selby, Katherine Anne [orcid.org/0000-0002-3055-2872](https://orcid.org/0000-0002-3055-2872) and Marchant, Robert [orcid.org/0000-0001-5013-4056](https://orcid.org/0000-0001-5013-4056) (2018) Holocene mangrove dynamics and relative sea-level changes along the Tanzanian coast, East Africa. *Estuarine coastal and shelf science*. pp. 105-117. ISSN 0272-7714

<https://doi.org/10.1016/j.ecss.2018.07.004>

---

**Reuse**

This article is distributed under the terms of the Creative Commons Attribution-NonCommercial-NoDerivs (CC BY-NC-ND) licence. This licence only allows you to download this work and share it with others as long as you credit the authors, but you can't change the article in any way or use it commercially. More information and the full terms of the licence here: <https://creativecommons.org/licenses/>

**Takedown**

If you consider content in White Rose Research Online to be in breach of UK law, please notify us by emailing [eprints@whiterose.ac.uk](mailto:eprints@whiterose.ac.uk) including the URL of the record and the reason for the withdrawal request.

1  
2  
3  
4 1 Holocene mangrove dynamics and relative sea-level changes along the Tanzanian  
5  
6 2 coast, East Africa

7  
8 3 Paramita Punwong<sup>1, 2\*</sup>, Katherine Selby<sup>3</sup>, Rob Marchant<sup>2</sup>  
9

10 4

11  
12 5 <sup>1</sup> Faculty of Environment and Resource Studies, Mahidol University, Nakhon  
13  
14 6 Pathom, 73170, Thailand

15  
16 7 <sup>2</sup> York Institute of Tropical Ecosystems, Environment Department, University of  
17  
18 8 York, York YO10 5NG, UK

19  
20 9 <sup>3</sup> Environment Department, University of York, York YO10 5NG, UK  
21  
22

23 10

24  
25 11 **Abstract** There is continued uncertainty regarding the rate, timing, duration and  
26  
27 12 direction of Holocene sea-level for the Indian Ocean, and indeed the wider  
28  
29 13 tropical realm. We present the first synthesis, and a new chronology, for  
30  
31 14 Holocene relative sea-level (RSL) using a range sediment cores retrieved from  
32  
33 15 mangrove ecosystems in three locations along coastal Tanzania. This study  
34  
35 16 applies the relationship of ratios between the key mangrove taxa of  
36  
37 17 *Sonneratia:(Bruguiera/Ceriops)* (S/BC) (ranging from 0 – 22.9) and  
38  
39 18 *Sonneratia:Rhizophora* (S/R) (ranging from 0 – 2.29), vegetation and altitude to  
40  
41 19 interpret mangrove dynamics and refine the vertical errors associated with relative  
42  
43 20 sea level change. The variations in mangrove taxa ratios in the sediment cores  
44  
45 21 obtained from each site shows mangrove development at different periods during  
46  
47 22 the Holocene from around 7900 cal yr BP. An early to mid-Holocene RSL rise  
48  
49 23 occurred from ~7900 to ~4600 cal yr BP that may have reached a higher level  
50  
51 24 than present. A lower RSL occurred after 4600 cal yr BP, resulting in mangroves  
52  
53 25 retreating seaward at all three study locations, before a low magnitude RSL rise  
54  
55  
56  
57  
58  
59  
60

61  
62  
63  
64 26 occurred between 4400 and 2000 cal yr BP. Another RSL rise is recorded at ~  
65  
66 27 500 cal yr BP before falling to a level lower than present at ~100 cal yr BP. There  
67  
68 28 is evidence of a recent RSL rise recorded from mangrove ratios during the last  
69  
70 29 century. In addition, the sedimentation rates among sites are relatively different  
71  
72 30 due to different altitudinal ranges with freshwater input, sediment supply and  
73  
74 31 progradation having significantly more effect in the Rufiji Delta (2.1-10.9 mm cal  
75  
76 32 yr<sup>-1</sup>) than at the Zanzibar sites (0.3-6.6 mm cal yr<sup>-1</sup>).  
77  
78  
79 33

80  
81 34 Keywords: Indian Ocean, pollen-vegetation relationships, far-field locations,  
82  
83 35 Zanzibar, Rufiji Delta  
84

85 36

86  
87 37 \*Corresponding author.  
88

89 38 E-mail: [punnbio@gmail.com](mailto:punnbio@gmail.com); [paramita@mahidol.edu](mailto:paramita@mahidol.edu)  
90  
91  
92  
93  
94  
95  
96  
97  
98  
99  
100  
101  
102  
103  
104  
105  
106  
107  
108  
109  
110  
111  
112  
113  
114  
115  
116  
117  
118  
119  
120

121  
122  
123  
124 39 1. Introduction  
125

126 40 Relative sea-level (RSL) (the height of the ocean with respect to the  
127  
128 41 surface of the solid Earth) has fluctuated over time that has resulted in  
129  
130 42 geophysical and ecological changes (Pirazzoli, 1991). Far-field sites, located at a  
131  
132 43 distance from the major ice sheets, are important locations for reconstructing RSL  
133  
134 44 changes. Far-field locations can provide important constraints on global RSL  
135  
136 45 change when combined with more intensively studied temperate areas, where  
137  
138 46 coastal adjustments following removal of ice loading are most acute, especially  
139  
140  
141 47 during the mid and late Holocene (Milne and Mitrovica, 2008).  
142

143 48 Holocene RSL changes in far-field locations result from eustatic changes,  
144  
145 49 equatorial syphoning and hydro-isostasy (continental levering) (Mitrovica and  
146  
147 50 Milne, 2002; Milne and Mitrovica, 2008). Equatorial ocean syphoning results  
148  
149 51 from collapsing forebulges at the near-field continental margins that cause RSL  
150  
151 52 fall to be recorded in far-field locations (Mitrovica and Peltier, 1991). Continental  
152  
153 53 levering occurs when there is water loading due to deglaciation, that causes  
154  
155 54 continental subsidence and an uplift of the adjacent continents, inducing RSL fall  
156  
157  
158 55 at areas distant from the continental margins (Lambeck and Nakada, 1990;  
159  
160 56 Mitrovica and Milne, 2002; Gehrels and Long, 2008). RSL records from far-field  
161  
162 57 locations have been produced from various locations including the Indian Ocean  
163  
164 58 (Katupotha and Fujiwara, 1988; Banjeree, 2000), Southeast Asia (Hanebuth et al.,  
165  
166 59 2000; Horton et al., 2005; Bird et al., 2007) and Australia (Lambeck and Nakada,  
167  
168 60 1990; Larcombe et al., 1995; Lewis et al., 2013). Holocene RSL changes have  
169  
170 61 been reconstructed from Australia using a range of coastal and coral reef proxies;  
171  
172 62 some studies suggest a highstand at ~6000 cal yr BP (Lambeck and Nakada, 1990;  
173  
174 63 Larcombe et al., 1995), whereas others indicate a later highstand around 3900 cal  
175  
176  
177  
178  
179  
180

181  
182  
183  
184 64 yr BP (Baker et al., 2001). A review of geo-chronological data from along the  
185  
186 65 southeast coast of Australia, indicates a highstand from 7700 cal yr BP that lasted  
187  
188 66 until about 2000 cal yr BP, before falling to the present-day level (Sloss et al.,  
189  
190 67 2007). In the northern Indian Ocean, two mid-late Holocene highstands, one at  
191  
192 68 7300 cal yr BP and another at 4300 cal yr BP, have been recorded from beach  
193  
194 69 ridges and coral terraces along the east coast of India (Banerjee, 2000). These  
195  
196 70 highstands were also recorded from corals and marine shells along the southwest  
197  
198 71 and south coasts of Sri Lanka (Katupotha and Fujiwara, 1988) occurring at 6500  
199  
200  
201 72 cal yr BP and 3200 cal yr BP.

202  
203 73 Clearly far-field RSL records are of immense value for understanding and  
204  
205 74 constraining sea level records but there is a range of timings and duration of these.  
206  
207 75 In this paper we present evidence of RSL changes derived from three mangrove  
208  
209 76 sediment records (Punwong et al., 2012; 2013a; 2013b) from sites on the  
210  
211 77 Tanzanian coast. Combined, these data provide the first sea-level curve and a  
212  
213 78 refined chronology for Holocene RSL and coastal changes for Tanzania. This  
214  
215 79 study also uses the relationship between ratios of key mangrove taxa, vegetation  
216  
217 80 and altitude to interpret mangrove dynamics and refine the vertical errors of RSL  
218  
219 81 change. Holocene RSL changes are integrated with existing RSL reconstructions  
220  
221 82 from the region to develop a reconstruction of Holocene RSL changes across the  
222  
223 83 Southwest Indian Ocean.

224  
225  
226 84

### 227 228 85 1.1. Sea-level history in the southwest Indian Ocean

229  
230 86 The record of Holocene RSL change along the East African coast, situated  
231  
232 87 in the tectonically stable (Woodroffe and Horton, 2005) Southwest Indian Ocean,  
233  
234 88 is poorly constrained (Pirazzoli, 1991; Camoin et al., 2004). Reconstructed RSL  
235  
236  
237  
238  
239  
240

241  
242  
243  
244 89 changes are available from only a few locations and use a range of different  
245  
246 90 proxies (Figure 1a). Previous studies of RSL change on the continental coasts of  
247  
248 91 east and southeast Africa (Mozambique and South Africa) indicate that RSL rose  
249  
250 92 rapidly during the early Holocene and reached the present level by the mid  
251  
252 93 Holocene (Jaritz et al., 1977, Ramsay, 1995; Ramsay and Cooper, 2002; Norström  
253  
254 94 et al., 2012). Mid Holocene highstands of up to 3.5 m above the present level  
255  
256 95 were recorded by 5000 cal yr BP, followed by subsequent falls to the present level  
257  
258 96 in the late Holocene. A different RSL reconstruction derived from coral from the  
259  
260 97 offshore islands (Mauritius, Mayotte and Réunion Island) shows that a rapid RSL  
261  
262 98 rise occurred during the early Holocene reaching present level at ~3000 cal yr BP  
263  
264 99 with no evidence for a mid Holocene highstand (Camoin et al., 1997; 2004;  
265  
266 100 Colonna et al., 1997; Zinke et al., 2003). Although all RSL studies within this  
267  
268 101 region record an early Holocene RSL rise, there is considerable uncertainty on the  
269  
270 102 amplitude and timing of this. The varied environmental settings and distances  
271  
272 103 from formerly glaciated areas would result in different isostatic contributions to  
273  
274 104 RSL changes. For example, it is thought that small offshore volcanic islands are  
275  
276 105 less affected by hydro-isostatic adjustment than those studies from continental  
277  
278 106 locations due to the effects of continental levering during the mid and late  
279  
280 107 Holocene (Camoin et al., 2004; Lambeck and Nakada, 1990; Mitrovica and  
281  
282 108 Milne, 2002; Milne and Mitrovica, 2008). The different proxies used make it  
283  
284 109 likely that the sea-level index points may not be comparable and some sea-level  
285  
286 110 index points may have large indicative ranges and different degrees of precision  
287  
288 111 (Jaritz et al., 1977; Ramsay, 1995; Ramsay and Cooper, 2002; Woodroffe and  
289  
290 112 Horton, 2005; Norström et al., 2012).

291  
292  
293  
294  
295 113  
296  
297  
298  
299  
300

301  
302  
303  
304 114 1.2. Mangrove as sea-level indicators  
305

306 115 Research on RSL reconstruction from far-field locations has traditionally  
307  
308 116 focused on coring and dating corals (Pirazzoli, 1988; Fairbanks, 1989; Colonna et  
309  
310 117 al., 1997; Camoin et al., 1997, 2004). However, sediments that accumulate within  
311  
312 118 mangrove ecosystems can also be used to reconstruct RSL and coastal changes.  
313  
314 119 Mangrove ecosystems are found in coastal tropical regions along the margins of  
315  
316 120 the sea and lagoons; they are characterised by evergreen trees and shrubs that are  
317  
318 121 physiologically and morphologically adapted to grow in the sub-tropical to  
319  
320 122 tropical intertidal zone between mean sea level and the high water of spring tide  
321  
322 123 (Woodroffe and Grindrod, 1991; Blasco et al., 1996; Ellison and Farnsworth,  
323  
324 124 2001; Ellison, 2008). Mangrove ecosystems respond to changes in sea level by  
325  
326 125 migrating landwards with a rise in sea level or seawards with a fall (Gilman et al.,  
327  
328 126 2008). Mangrove community composition is able to keep pace with sea-level  
329  
330 127 changes (McIvor et al., 2013). For mangroves to be able to withstand sea level  
331  
332 128 rise, the rates of sedimentary accretion within the mangrove has to be equivalent  
333  
334 129 to the rate of sea-level rise (Ellison, 2015), otherwise mangroves may undergo *in*  
335  
336 130 *situ* drowning leading to weakened root structures, dieback and disappearance  
337  
338 131 (Gilman et al., 2008).  
339  
340  
341

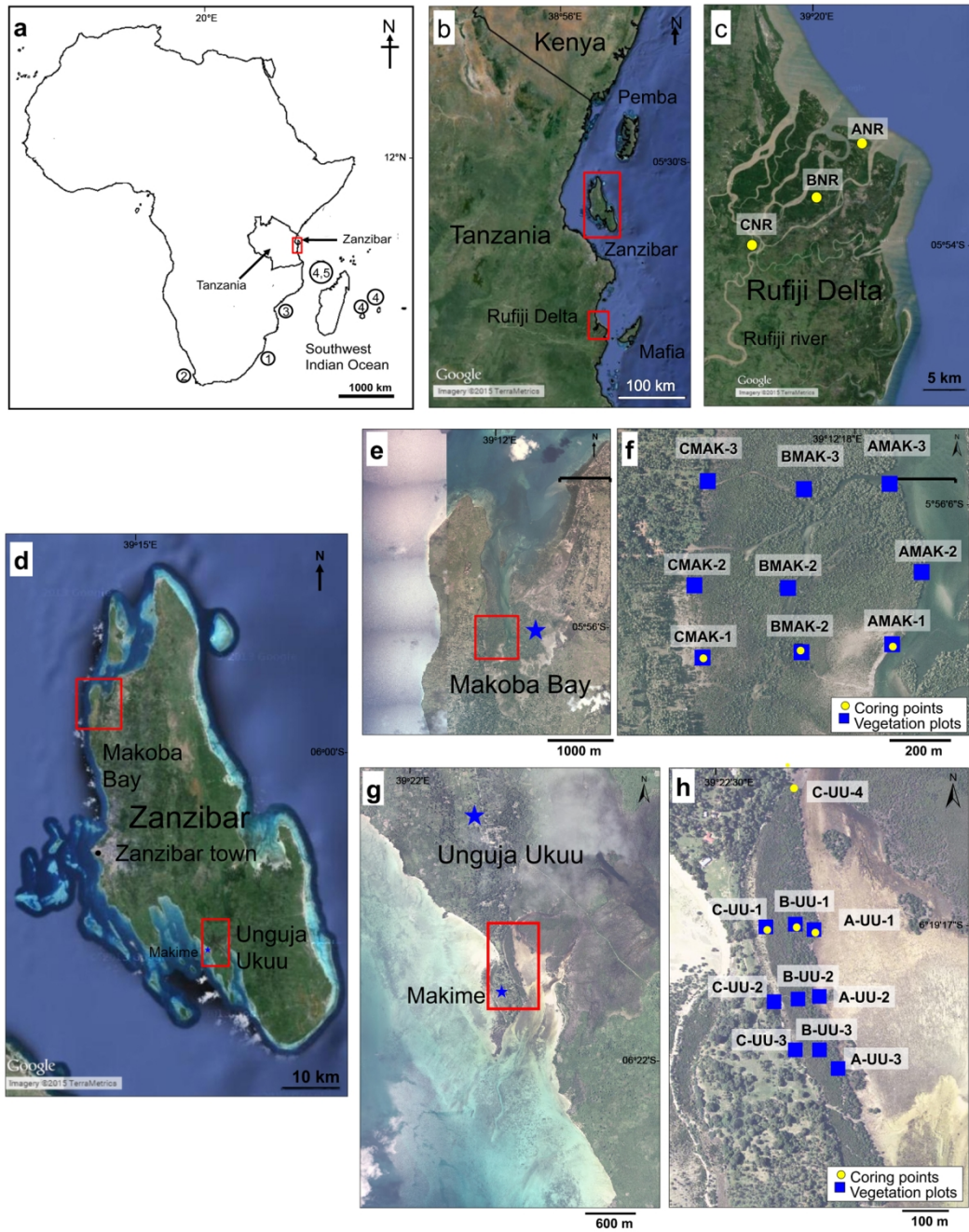
342 132 Santisuk (1983) and Watson (1928) classified mangroves into a series of  
343  
344 133 inundation class zones according to ecological preference to monthly inundation  
345  
346 134 frequency. *Rhizophora mucronata*, *Avicennia marina*, *Sonneratia alba*, *Bruguiera*  
347  
348 135 *gymnorhiza* and *Ceriops tegal* are classified as true mangroves or mangroves.  
349  
350 136 The term true mangroves are also defined as mangroves representing trees and  
351  
352 137 shrubs growing in the areas inundated by the normal to all high tides. Back  
353  
354 138 mangroves such as *Heritiera littoralis* and *Acrostichum aureum* are plants  
355  
356  
357  
358  
359  
360

361  
362  
363  
364 139 growing in the areas inundated by the sea only during spring high tides,  
365  
366 140 exceptional high tides, or during cyclones. The dominance of mangrove species  
367  
368 141 which occurs in zones throughout the mangrove ecosystem can thus be an  
369  
370 142 indicator of sea-level fluctuations by comparing the relationships between  
371  
372 143 contemporary vegetation assemblages and their inundation frequency with respect  
373  
374 144 to sea level.

375  
376 145 Mangrove pollen has previously been used to reconstruct compositional  
377  
378 146 changes in mangrove ecosystems (e.g. Cohen et al., 2005; Horton et al., 2005;  
379  
380 147 Vedel et al., 2006; Tossou et al., 2008; Hait and Behling, 2009) including in East  
381  
382 148 Africa (Punwong et al., 2012; 2013a; 2013b). Engelhart et al. (2007) developed a  
383  
384 149 transfer function from a modern analogue of mangrove surface pollen  
385  
386 150 assemblages that has been used to predict the palaeo mangrove elevation with  
387  
388 151 precision of  $\pm 0.22$  m. A contemporary study into the relationships between  
389  
390 152 mangrove pollen in surface sediment samples and the composition of the  
391  
392 153 vegetation indicated that majority of pollen was local in origin reflecting  
393  
394 154 vegetation in close proximity to the sampling sites (Punwong et al., 2013a,  
395  
396 155 2013b). Pollen accumulated in sediments underlying mangroves, in combination  
397  
398 156 with an understanding of the present relationship of mangrove composition to the  
399  
400 157 altitude of present sea level, can be used to reconstruct RSL fluctuations (Ellison,  
401  
402 158 1989; 2005; 2008; Punwong et al., 2012; 2013a; 2013b).  
403  
404  
405  
406  
407  
408  
409  
410  
411  
412  
413  
414  
415  
416  
417  
418  
419  
420



421  
422  
423  
424  
425  
426  
427  
428  
429  
430  
431  
432  
433  
434  
435  
436  
437  
438  
439  
440  
441  
442  
443  
444  
445  
446  
447  
448  
449  
450  
451  
452  
453  
454  
455  
456  
457  
458  
459  
460  
461  
462  
463  
464  
465  
466  
467  
468  
469  
470  
471  
472  
473  
474  
475  
476  
477  
478  
479  
480



159

160 Figure 1. (a) Map of the Southwest Indian Ocean showing the location of  
161 Tanzania and previous sea level studies: (1) Ramsay and Cooper (2002), (2)  
162 Compton (2001), (3) Jaritz et al. (1977), (4) Colonna et al. (1996); Camoin et al.  
163 (1997), (5) Zinke (2000); Zinke et al. (2003). (b) Map of the coast of Tanzania  
164 showing the location of the Rufiji Delta (c) and Zanzibar (d). Inset e, f, g and h  
165 show where the sedimentary cores were taken and the location of vegetation plots  
166 located in Makoba Bay and Unguja Ukuu respectively.

481  
482  
483  
484 167

485  
486 168 2. Study sites

487  
488 169

489  
490 170 2.1. Geology and geomorphology

491  
492 171 The three sites investigated are all characterised by mangrove forest and  
493  
494 172 located in the northern Rufiji Delta (Tanzanian mainland), Makoba Bay and  
495  
496 173 Unguja Ukuu (Unguja island, Zanzibar) (Figure 1b-h). The Rufiji Delta consists  
497  
498 174 of mangrove forest that grades into paddy fields at higher elevations and supports  
499  
500 175 the largest expanse of estuarine mangrove along the East African coast  
501  
502 176 (Nshubemuki, 1993; Fisher et al., 1994; Richmond et al., 2002; Masalu, 2003;  
503  
504 177 Mangora et al., 2016). The deltaic area is covered by fluvial sand, silt and clay  
505  
506 178 (Semesi, 1992) (Figure 1c). A series of sand spit islands and submerged sand bars  
507  
508 179 have formed parallel to the seaward margins (Fisher et al., 1994), while clayey  
509  
510 180 silts and silty clays containing organic matter characterise the mangrove  
511  
512 181 sediments. The average tidal range is 2 - 2.5 m and approximately 3.3 - 4.3 m on  
513  
514 182 high spring tides (Francis, 1992; Fisher et al., 1994; Richmond et al., 2002).

515  
516  
517 183 Unguja Island (Zanzibar) is located on the continental shelf some 40 km  
518  
519 184 from the mainland. The island has been periodically part of the mainland when  
520  
521 185 sea level was 30-40 m below present sea level and the last separation from the  
522  
523 186 mainland by sea-level inundation of the Zanzibar channel occurred at the end of  
524  
525 187 the Pleistocene to early Holocene (Prendergast et al., 2016). Most of Unguja  
526  
527 188 consists of Pleistocene reef limestone often outcropping on the east coast  
528  
529 189 (Shunula, 2002) with alluvial deposits locally present (Schlüter, 1997; Arthurton  
530  
531 190 et al., 1999) although there are no large rivers (Shunula, 2002). It is influenced by  
532  
533 191 a semi-diurnal tide, ranging from 2 m on neap tide to 4 m on spring tide  
534  
535  
536  
537  
538  
539  
540

541  
542  
543  
544 192 (Mwandya et al., 2010). The study areas are located in the northwest of Makoba  
545  
546 193 Bay (Figure 1d; 1e) and the east Makime headland of Unguja Ukuu (Figure 1d;  
547  
548 194 1g).

549  
550 195

## 552 196 2.2. Climate

554 197 The rainfall pattern within the Rufiji Delta and on Zanzibar is largely  
555  
556 198 controlled by the north and south migration of the Inter-tropical Convergence  
557  
558 199 Zone (ITCZ). For the Rufiji delta, the northeast monsoon prevails from December  
560  
561 200 to April bringing heavy rainfall (Goudie, 1996; Nicholson, 2001) and the  
562  
563 201 southeast monsoon dominates from May to November bringing less rainfall  
565  
566 202 (Fisher et al., 1994; Richmond et al., 2002). The average annual rainfall is about  
567  
568 203 1200 mm yr<sup>-1</sup> (Semesi, 1992) and the temperature range throughout the year is 24  
569  
570 204 - 31 °C (Richmond et al., 2002). For Zanzibar, the northeast and southeast  
571  
572 205 monsoons bring the long rains from March to May and short rains from October  
573  
574 206 to December (Machiwa and Hallberg, 1995; Mwandya et al., 2010). The mean  
575  
576 207 annual rainfall is about 1500 -1800 mm yr<sup>-1</sup> (Knopp et al., 2008) and the average  
577  
578 208 temperature range throughout the year is about 27 - 30 °C (Machiwa and  
579  
580 209 Hallberg, 1995).

581  
582 210

## 584 211 3. Methodology

585  
586 212

### 588 213 3.1. Coring

590 214 Three sediment cores were retrieved from each site at a seaward, central and  
591  
592 215 landward location using a Russian corer along a transect perpendicular to the  
593  
594 216 coastline through the centre of mangrove forests to reduce the influence of local  
595  
596  
597  
598  
599  
600

601  
602  
603  
604 217 land-based edge effects such as erosion or progradation from creeks (Ellison,  
605  
606 218 2008). The core depths varied between 1 to 4.5 m (Table 1) and each site was  
607  
608 219 cored until the sediment became impenetrable or bedrock was reached (Punwong  
609  
610 220 et al., 2012; 2013a; 2013b). The transect length varied depending on the nature of  
611  
612 221 the environmental setting and the extent of the mangrove area; this extended along  
613  
614 222 20 km in the northern Rufiji Delta (ANR, BNR, CNR), 600 m in Makoba Bay  
615  
616 223 (AMAK-1, BMAK-1, CMAK-1) and 80 m at Unguja Ukuu (A-UU-1, B-UU-1, C-  
617  
618 224 UU-1) (Figures 1c; 1f; 1h, Table 1). An additional sediment core was retrieved  
619  
620 225 from Unguja Ukuu (C-UU-4) at a location away from the transect as it represents  
621  
622 226 a longer sediment record than the other three cores.

### 625 227 3.2. Vegetation plots

627 228 To study the relationship between mangrove species composition, pollen  
628  
629 229 accumulating in the sediment and RSL, nine 20 m<sup>2</sup> vegetation plots were set up to  
630  
631 230 establish species percentages along an altitudinal gradient. At the three sites, there  
632  
633 231 was considerable variation in the horizontal distance covered to accommodate the  
634  
635 232 full range of the upper and the lower limits of mangroves. In the Rufiji Delta, the  
636  
637 233 vegetation survey transect along the large riverine mangrove system with  
638  
639 234 freshwater inputs covered 20 km. As the consequence, we were not able to carry  
640  
641 235 out adequate vegetation surveys and to set up plots within the restricted fieldwork  
642  
643 236 time frame. On Zanzibar the transects extended between 80 to 600 m of fringing  
644  
645 237 mangroves characterised by a similar composition across the three sites. Given  
646  
647 238 variations in the horizontal distance and vertical range, the mangrove gradient in  
648  
649 239 Zanzibar is considered to be steeper than the Rufiji Delta. A more detailed study  
650  
651 240 at both sites in Zanzibar allowed the ecosystem and structural composition at  
652  
653 241 different levels of sea-level inundation to be determined and inform the  
654  
655  
656  
657  
658  
659  
660

661  
662  
663  
664 242 reconstruction of past RSL fluctuations. Vegetation in nine 20 m<sup>2</sup> nested quadrats  
665  
666 243 was surveyed and recorded and surface sediment samples were collected (Figures  
667  
668 244 1f, 1h) from three seaward, three central and three landward sites, then considered  
669  
670 245 to be an upper intertidal, a middle intertidal and a lower intertidal mangrove  
671  
672 246 classes, respectively. Five cm<sup>3</sup> of surface samples from the four corners and centre  
673  
674 247 of each plot were collected and subsequently used to study the relationship  
675  
676 248 between pollen presence and vegetation coverage. Altitudinal heights were  
677  
678 249 obtained using a differential GPS (dGPS model Leica TCRA total station and  
679  
680  
681 250 Leica System 500 base and receiver with a manufacturer quoted vertical precision  
682  
683 251 of  $\pm 0.001$  m). Initial calibration of the dGPS occurred against recognised  
684  
685 252 National Datum benchmarks and subsequently all coring sites, vegetation plots  
686  
687 253 and full range of mangrove sites were levelled and calibrated to mean tide level  
688  
689 254 (MTL) (based on Admiralty Tide Tables, 2014). These altitudes were determined  
690  
691 255 relative to a benchmark at Kibiti for the Rufiji Delta using a known actual base  
692  
693 256 station Triangulation point (TTP 353) and the Ministry of Lands and the  
694  
695 257 Environment Benchmark (Zanzibar).

### 698 258

### 700 259 3.3. Palaeoecological analysis

702 260 The cores were sub-sampled every 10 cm and the volume of each subsample  
703  
704 261 was approximately 2 cm<sup>3</sup> for pollen analysis (Punwong et al., 2012; 2013a;  
705  
706 262 2013b). The relationship between pollen assemblages and vegetation composition  
707  
708 263 was determined using three pollen association indices that reflect how accurately  
709  
710 264 pollen types reflect the abundance of their parent plant (Davis, 1984). The three  
711  
712 265 indices are ‘association index’ representing similar presence of the pollen and the  
713  
714 266 associated plant in the vegetation, ‘under-representation index’ representing

721  
722  
723  
724 267 pollen percentages that are much lower than plant percentages, and ‘over-  
725  
726 268 representation index’ representing pollen percentages that exceed plant  
727  
728 269 percentages (Davis, 1984). Pearson’s Correlation Coefficients were used to  
729  
730 270 describe the relationship between pollen percentages extracted from the surface  
731  
732 271 sediment and plant percentages from the nine vegetation plots in Makoba Bay and  
733  
734 272 Unguja Ukuu.

736  
737 273

#### 738 274 3.4. Chronology

740  
741 275 Twenty-six bulk sediment samples were selected for AMS dating and  
742  
743 276 submitted to the Radiocarbon Dating Laboratories at the University of Waikato,  
744  
745 277 New Zealand and the CHRONO Centre, Queen’s University Belfast, UK. At the  
746  
747 278 start of the laboratory work, dates were obtained from the base of the core with  
748  
749 279 targeted dating from different stratigraphic boundaries and key biostratigraphical  
750  
751 280 horizons occurring as the research developed. Additionally, nine dates from  
752  
753 281 AMAK-1 and BMAK-1 cores were obtained on organic concentrate samples  
754  
755 282 following Woodroffe et al. (2015a). Each 1 cm<sup>3</sup> bulk sediment was deflocculated  
756  
757 283 using Na<sub>4</sub>P<sub>2</sub>O<sub>4</sub>/ NaOH, heated with 10% HCl and sieved through a 10, 63 and 90  
758  
759 284 µm mesh. The 10-63 µm sieving fraction was selected for dating as it contained  
760  
761 285 fine organic material and pollen (Woodroffe et al., 2015a). The organic  
762  
763 286 concentrate samples were submitted for dating to the Natural Environment  
764  
765 287 Research Council (NERC) Radiocarbon Facility (East Kilbride) for AMS dating  
766  
767 288 (NERC Radiocarbon Facility Allocation 1608.0312). All dates were calibrated  
768  
769 289 using the southern hemisphere calibration Shcal04 curve (McCormac et al., 2004)  
770  
771 290 using the software OxCal v4.10 (Bronk-Ramsey, 2009).  
772  
773 291

774  
775 291

721  
722  
723  
724  
725  
726  
727  
728  
729  
730  
731  
732  
733  
734  
735  
736  
737  
738  
739  
740  
741  
742  
743  
744  
745  
746  
747  
748  
749  
750  
751  
752  
753  
754  
755  
756  
757  
758  
759  
760  
761  
762  
763  
764  
765  
766  
767  
768  
769  
770  
771  
772  
773  
774  
775  
776  
777  
778  
779  
780

781  
782  
783  
784 292 4. Results  
785

786 293

787  
788 294 4.1. Stratigraphy  
789

790 295 Detailed stratigraphic descriptions and diagrams have been previously  
791  
792 296 published (Punwong et al., 2012; 2013; 2013b). There were no abrupt  
793  
794 297 stratigraphic boundaries between the units; they were gradational in all ten cores.  
795  
796 298 The basal unit of BNR and CNR in the northern Rufiji Delta was comprised of  
797  
798 299 organic matter and silt (Punwong et al., 2012). Organic matter amount, including  
799  
800 300 root fragments, increased towards the top of the cores where wood and bark  
801  
802 301 fragments were also present.  
803

804  
805 302 In the three cores retrieved from Makoba Bay, the deepest sediment was  
806  
807 303 grey silt with some shell fragments (Punwong et al., 2013b). In cores AMAK-1  
808  
809 304 and BMAK-1 the silt unit was overlain by a peat unit containing woody root  
810  
811 305 fragments and fine sand. Sand was found in the uppermost unit of all three cores.  
812

813 306 The basal unit of A-UU-1, B-UU-1 C-UU-1 sediment cores from Unguja  
814  
815 307 Ukuu was grey sand and silt with silt as the basal unit in C-UU-4 (Punwong et al.,  
816  
817 308 2013a). All basal units were overlain by peat with woody root fragments. Some  
818  
819 309 small shell fragments were also found in this unit in A-UU-1 and B-UU-1. Peat  
820  
821 310 layers with sand and small fragments of woody plant roots alternated with organic  
822  
823 311 sand layers throughout the sediment column in all four cores. Sand containing  
824  
825 312 small fragments of woody plant root formed the top unit of B-UU-1, C-UU-1, and  
826  
827 313 C-UU-4 while silt characterised the top unit of A-UU-1.  
828

829  
830 314

831  
832 315 4.2. Pollen analysis and vegetation survey  
833  
834  
835  
836  
837  
838  
839  
840

841  
842  
843  
844 316 Fossil pollen and spores were identified and placed into five main  
845  
846 317 ecological groups: mangroves, back mangroves, terrestrial herbaceous,  
847  
848 318 pteridophytes and unidentifiable pollen; the first two (mangroves, back  
849  
850 319 mangroves), denote a tolerance to sea-water inundation (Punwong et al., 2012;  
851  
852 320 2013a; 2013b). Terrestrial taxa consisted solely of terrestrial herbaceous plants  
853  
854 321 such as grasses and sedges that are not tolerant of salinity. An understanding of  
855  
856 322 the contemporary mangrove species within the zones is used to underpin the  
857  
858 323 interpretation of ecosystem and environmental changes through the fossil record.  
859  
860  
861 324 Nine mangrove species found in Tanzania within a zonation scheme developed  
862  
863 325 through a combination of Watson's (1928) and Santisuk's (1983) inundation  
864  
865 326 classes (mangroves and back mangroves) and field-based observations of modern  
866  
867 327 ecological occurrences of mangrove taxa (Figure 2a) (Punwong et al., 2012;  
868  
869 328 2013a; 2013b) are therefore used as a modern analogue of mangrove pollen to  
870  
871 329 interpret sea level. Low mangrove diversities and a linear relationship between  
872  
873 330 contemporary mangrove habitat and inundation frequency negates the need for the  
874  
875 331 use of transfer functions (Ellison, 1989; Engelhart et al., 2007).

877  
878 332 Contemporary vegetation assemblages observed in the field based on  
879  
880 333 Watson and Santisuk (1928) classes revealed a distinct vertical relationship with  
881  
882 334 present sea level. The altitude of the upper and lower limits of the mangrove areas  
883  
884 335 was +1.67 m to +3.47 m mean tide level (MTL) in the northern Rufiji Delta, -1.63  
885  
886 336 m to +1.47 m MTL in Makoba Bay, and -0.03 m to +1.87 m MTL at Unguja  
887  
888 337 Ukuu. The altitudinal variation of the upper and lower limits of the mangrove  
889  
890 338 areas at the three sites is due to different mangrove systems and environmental  
891  
892 339 settings. In the northern Rufiji Delta, an estuarine mangrove ecosystem exists  
893  
894 340 while at Unguja Ukuu and Makoba Bay, fringe mangroves with less freshwater



901  
902  
903  
904 341 input are found. For Makoba Bay we acknowledge it is unusual for mangroves to  
905  
906 342 grow at -1.63 m MTL and is most likely caused by the geomorphology of the tidal  
907  
908 343 creek system that allows seaward mangrove species, e.g. *Sonneratia alba*, to  
909  
910 344 colonise altitudes below MTL.

912 345 The indices of pollen association (Davis, 1984) and correlation between  
913  
914 346 the contemporary mangrove pollen records and contemporary vegetation showed  
915  
916 347 that fossil mangrove pollen in Zanzibar have a close correlation between  
917  
918 348 representivity in pollen spectra and the actual vegetation and can be used to  
919  
920 349 reconstruct coastal ecosystem dynamics (Punwong et al., 2013a; 2013b).

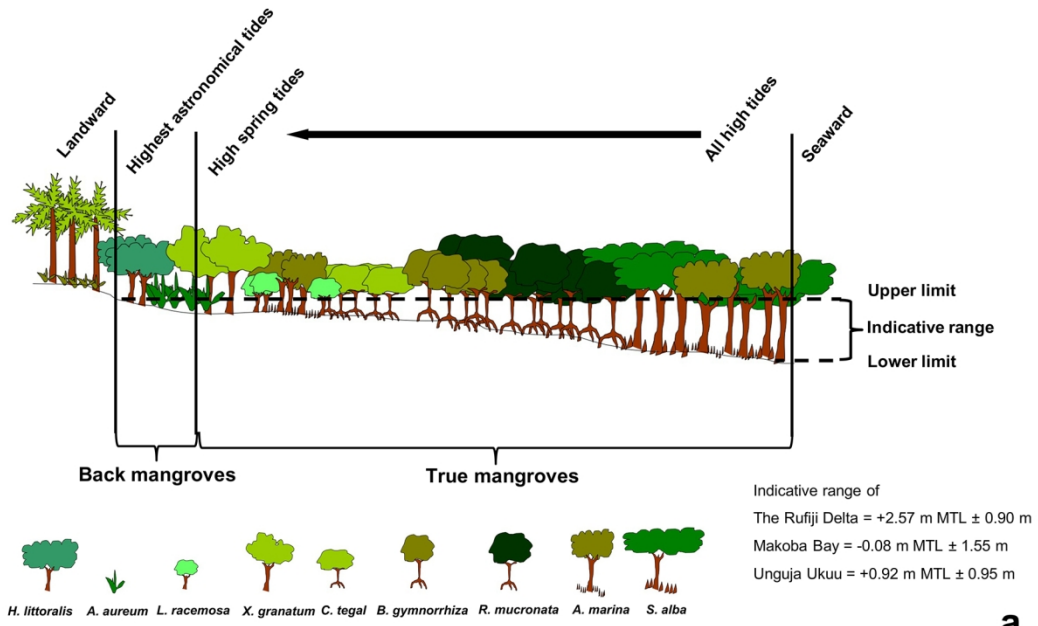
922 350 Strikingly, there are some notable changes between the percentages of *Sonneratia*  
923  
924 351 *alba* and *Bruguiera/Ceriops* pollen throughout Zanzibar cores. At the present-day  
925  
926 352 *Sonneratia alba* and *Bruguiera/Ceriops* appear at different altitudes; *Sonneratia*  
927  
928 353 *alba* occurs in the lower intertidal zone whilst *Bruguiera* and *Ceriops* occur at  
929  
930 354 higher intertidal areas. The relative pollen ratios of  
931  
932 355 *Sonneratia:(Bruguiera/Ceriops)* (S/BC ratio) and *Sonneratia:Rhizophora* (S/R  
933  
934 356 ratio) of the surface samples from each vegetation plot vary with altitudinal  
935  
936 357 gradient (Table 2). An increase in the ratios of S/BC and S/R indicates a decrease  
937  
938 358 in altitude of the mangrove ecosystem and associated sea level (Table 2). These  
939  
940 359 ratios are applied to infer the mangrove altitude shift within the upper and lower  
941  
942 360 altitudinal limits of the Makoba Bay and Unguja Ukuu study areas as a modern  
943  
944 361 analogue of altitude mangrove classes (Table 2). In Makoba, the S/BC ratios of  
945  
946 362 5.4 – 22.8 and the S/R ratios of 0.37 – 2.29 represent lower intertidal mangroves;  
947  
948 363 the S/BC ratios of 0.2 – 5.4 and the S/R ratios of 0.04 – 2.29 represent middle  
949  
950 364 intertidal mangroves; the S/BC ratios of 0 – 0.2 and S/R ratios of 0 – 0.04  
951  
952 365 represent higher intertidal mangroves. At Unguja Ukuu, the S/BC ratios of 0.17 –  
953  
954  
955  
956  
957  
958  
959  
960

961  
962  
963  
964 366 2.23 and the S/R ratios of 0.20– 0.59 represent lower intertidal mangroves; the  
965  
966 367 S/BC ratios of 0 – 0.17 and the S/R ratios of 0 – 0.20 represent higher intertidal  
967  
968 368 mangroves.

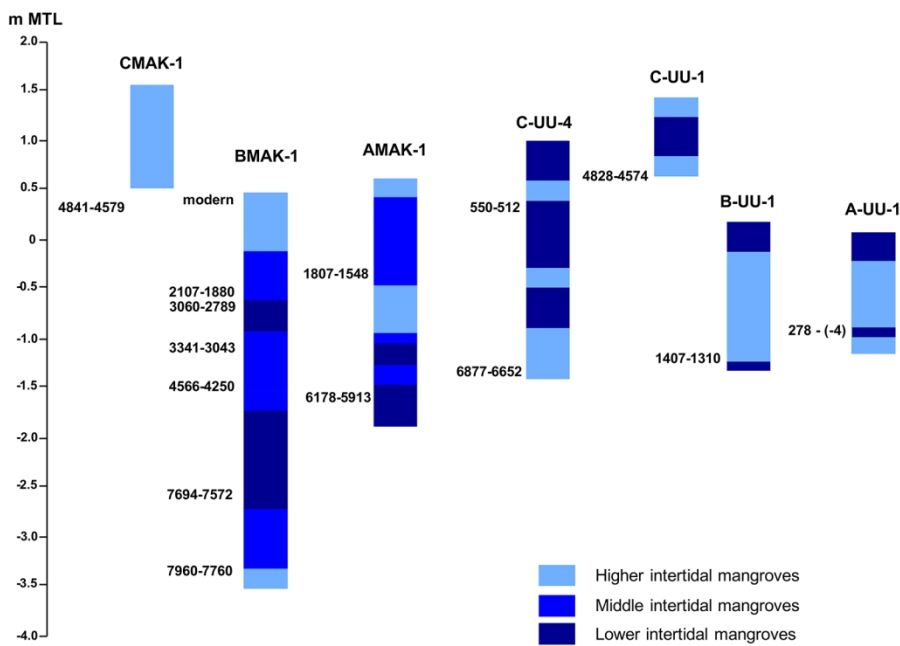
969  
970 369 Therefore, the pollen biostratigraphy as used in this study allows  
971  
972 370 correlation between horizons using the S/BC and S/R ratios of the surface samples  
973  
974 371 within the eighteen vegetation plots that were calculated and used to characterise  
975  
976 372 the mangrove position of the reconstructed past mangrove ecosystems. This  
977  
978 373 information is applied to the dated samples (Figure 2b).

979  
980  
981 374  
982  
983  
984  
985  
986  
987  
988  
989  
990  
991  
992  
993  
994  
995  
996  
997  
998  
999  
1000  
1001  
1002  
1003  
1004  
1005  
1006  
1007  
1008  
1009  
1010  
1011  
1012  
1013  
1014  
1015  
1016  
1017  
1018  
1019  
1020

1021  
1022  
1023  
1024  
1025  
1026  
1027  
1028  
1029  
1030  
1031  
1032  
1033  
1034  
1035  
1036  
1037  
1038  
1039  
1040  
1041  
1042  
1043  
1044  
1045  
1046  
1047  
1048  
1049  
1050  
1051  
1052  
1053  
1054  
1055  
1056  
1057  
1058  
1059  
1060  
1061  
1062  
1063  
1064  
1065  
1066  
1067  
1068  
1069  
1070  
1071  
1072  
1073  
1074  
1075  
1076  
1077  
1078  
1079  
1080



a



b

375

376 Figure 2. (a) Summary cross section showing typical mangrove zonation and  
 377 response of this to RSL change in Tanzania developed from Watson's (1928) and  
 378 Santisuk's (1983) inundation classes and field observations with its indicative  
 379 range. Figure 2. (b) Biostratigraphy of core sites from Makoba Bay and Unguja  
 380 Ukuu showing paleoenvironmental interpretation in terms of mangrove position

1081  
 1082  
 1083  
 1084 as lower, middle, higher inferred from the ratios of S/BC and S/R. All ages are in  
 1085  
 1086 cal yr BP developed from Punwong et al. (2013a; 2013b).  
 1087

| Site                  | Core      | Altitude (m MTL) | <sup>14</sup> C yr BP    | (2σ) Calibrated age range yr BP | Indicative meaning (m MTL) derived from full range of mangrove | RSL (m MTL) derived from full range of mangroves | Mangrove classes with altitudinal range (interpolated from Fig. 2b) | Indicative meaning (m MTL) derived from pollen ratios | RSL (m MTL) derived from pollen ratios | Decompaction correction | Sea-level tendency |
|-----------------------|-----------|------------------|--------------------------|---------------------------------|--|--|---|---|--|-------------------------|--------------------|
| Northern Rufiji Delta | ANR       | 1.61             | 392 ± 30                 | 493-324                         |  |  |   |   |  |                         |                    |
|                       | BNR       | 3.22             | > 1950 A.D.              |                                 |  |  |   |   |  |                         |                    |
|                       |           | 2.95             | Failure to make graphite |                                 |  |  |   |   |  |                         |                    |
|                       |           | 2.34             | 4167 ± 30                | 4821-4453                       | 2.57 ± 0.9   | -0.23 ± 0.9                                      | n/a   | n/a   | n/a                                    | 1.03                    | rise               |
|                       |           | 0.61             | 4751 ± 30                | 5579-5318                       | 2.57 ± 0.9   | -1.96 ± 0.9                                      | n/a   | n/a   | n/a                                    | 0.51                    | rise               |
|                       |           | -0.96            | 4931 ± 30                | 5711-5486                       | 2.57 ± 0.9   | -3.59 ± 0.9                                      | n/a   | n/a   | n/a                                    | 0.02                    | rise               |
|                       | CNR       | 2.33             | > 1950 A.D.              |                                 |  |  |   |   |  |                         |                    |
|                       | 1.06      | 884 ± 31         | 799-680                  | 2.57 ± 0.9                      | -1.51 ± 0.9  | n/a  | n/a   | n/a   | 0.62                                   | fall                    |                    |
| -0.97                 | 1292 ± 30 | 1264-1071        | 2.57 ± 0.9               | -3.54 ± 0.9                     | n/a  | n/a  | n/a   | 0.02  | fall                                   |                         |                    |
| Makoba Bay            | AMAK-1    | -0.37*           | 1803 ± 36                | 1807-1548                       | -0.08 ± 1.55   | -0.29 ± 1.55                                     | Middle intertidal (-1.14)-0.57                                      | -0.08 ± 0.86  | -0.29 ± 0.86                           | 0.46                    | rise               |
|                       |           | -0.41            | 1615 ± 24                | 1525-1385                       |  |  |   |   |  |                         |                    |
|                       |           | -1.55*           | 5290 ± 38                | 6178-5913                       | -0.08 ± 1.55   | -1.47 ± 1.55                                     | Lower intertidal (-1.61) - (-1.14)                                  | -0.08 ± 0.23  | -1.47 ± 0.23                           | 0.11                    | fall               |
|                       |           | -1.56            | 5078 ± 26                | 5892-5659                       |  |  |   |   |  |                         |                    |
|                       | BMAK-1    | 0.39*            | Modern                   |                                 | -0.08 ± 1.55   | 0.47 ± 1.55                                      | Higher intertidal 0.57-1.51   | -0.08 ± 0.47  | 0.47 ± 0.47                            | 1.19                    | fall               |
|                       |           | -0.54            | 3111 ± 24                | 3362-3167                       |  |  |   |   |  |                         |                    |
|                       |           | -0.55*           | 2072 ± 35                | 2107-1880                       | -0.08 ± 1.55   | -0.47 ± 1.55                                     | Middle intertidal (-1.14)-0.57                                      | -0.08 ± 0.86  | -0.47 ± 0.86                           | 0.91                    | fall               |
|                       | BMAK-1    | -0.64            | 1543 ± 25                | 1477-1305                       |  |  |   |   |  |                         |                    |
|                       |           | -1.16            | 1695 ± 50                | 1692-1408                       |  |  |   |   |  |                         |                    |
|                       |           | -1.17*           | 3053 ± 37                | 3341-3043                       | -0.08 ± 1.55   | -1.09 ± 1.55                                     | Middle intertidal (-1.14)-0.57                                      | -0.08 ± 0.86  | -1.09 ± 0.86                           | 0.73                    | rise               |
|                       |           | -1.53            | 309 ± 23                 | 443-289                         |  |  |   |   |  |                         |                    |
|                       |           | -1.54*           | 4024 ± 40                | 4566-4250                       | -0.08 ± 1.55   | -1.46 ± 1.55                                     | Middle intertidal (-1.14)-0.57                                      | -0.08 ± 0.86  | -1.46 ± 0.86                           | 0.61                    | rise               |
|                       |           | -2.78            | 6878 ± 36                | 7735-7582                       |  |  |   |   |  |                         |                    |
|                       |           | -2.79*           | 6847 ± 39                | 7694-7572                       | -0.08 ± 1.55   | -2.7 ± 1.55                                      | Low intertidal (-1.61) - (-1.14)                                    | -0.08 ± 0.23  | -2.70 ± 0.23                           | 0.24                    | rise               |
|                       |           | -3.52*           | 7092 ± 38                | 7960-7760                       | -0.08 ± 1.55   | -3.46 ± 1.55                                     | Middle intertidal (-1.14)-0.57                                      | -0.08 ± 0.86  | -3.46 ± 0.86                           | 0.01                    | rise               |
|                       |           | -3.54            | 7202 ± 30                | 8025-7872                       |  |  |   |   |  |                         |                    |
| CMAK-1                | 0.41      | 5200 ± 35        | 5991-5751                |                                 |  |  |   |   |  |                         |                    |
|                       | 0.18      | 4239 ± 37        | 4841-4579                |                                 |  |  |   |   |  |                         |                    |
|                       | -0.24     | 3117 ± 35        | 3376-3162                |                                 |  |  |   |   |  |                         |                    |
| Unguja Ukuu           | A-UU-1    | -0.84            | 169 ± 22                 | 278(-4)                         | 0.92 ± 0.95  | -1.76 ± 0.95                                     | Lower intertidal 0.01-0.21  | 0.92 ± 0.10   | -1.76 ± 0.10                           | 0.17                    | fall               |
|                       | B-UU-1    | -1.24            | 1534 ± 23                | 1407-1310                       | 0.92 ± 0.95  | -2.16 ± 0.95                                     | Higher intertidal 0.21-1.91   | 0.92 ± 0.85   | -2.16 ± 0.85                           | 0.04                    | fall               |
|                       | C-UU-1    | 0.57             | 4211 ± 25                | 4828-4574                       | 0.92 ± 0.95  | -0.35 ± 0.95                                     | Lower intertidal 0.01-0.21  | 0.92 ± 0.10   | -0.35 ± 0.10                           | 0.09                    | rise               |
|                       | C-UU-4    | 0.59             | >1950 AD                 |                                 |  |  |   |   |  |                         |                    |
|                       |           | 0.39             | 560 ± 19                 | 550-512                         | 0.92 ± 0.95  | -0.53 ± 0.95                                     | Lower intertidal 0.01-0.21  | 0.92 ± 0.10   | -0.53 ± 0.10                           | 0.47                    | fall               |
|                       |           | -1.29            | 5973 ± 36                | 6877-6652                       | 0.92 ± 0.95  | -2.21 ± 0.95                                     | Higher intertidal 0.21-1.91   | 0.92 ± 0.85   | -2.21 ± 0.85                           | 0.02                    | rise               |

1118 383

1119 384

1120 385 Table 1. List of radiocarbon dates derived from bulk samples and organic  
 1121 386 concentrates (marked with asterisks) from three sites. The calibrated ages are  
 1122 387 shown using the Shcal04 curve (McCormac et al., 2004) within the software  
 1123  
 1124  
 1125  
 1126  
 1127  
 1128  
 1129  
 1130  
 1131  
 1132  
 1133  
 1134  
 1135  
 1136  
 1137  
 1138  
 1139  
 1140

1141  
1142  
1143  
1144 388 OxCal v4.10 Bronk-Ramsey (2009). RSL dates are also depicted using the  
1145  
1146 389 indicative range derived from the upper and lower limits of modern mangrove  
1147  
1148 390 vegetation and altitudinal error derived from the full range of mangroves for the  
1149  
1150 391 Rufiji Delta and from the pollen ratios for Makoba and Unguja Ukuu.

| Site        | Plot   | Altitude of plot MTL (m) | Altitudinal range of mangrove classes | S/BC ratio | Range of S/BC ratios | S/R ratio | Range of S/R ratios | Mangrove classes  |
|-------------|--------|--------------------------|---------------------------------------|------------|----------------------|-----------|---------------------|-------------------|
| Makoba Bay  | AMAK-3 | -1.61                    | (-1.61) - (-1.14)                     | 22.8       | 5.4-22.8             | 2.29      | 0.37-2.29           | Lower intertidal  |
|             | AMAK-2 | -1.14                    |                                       | 5.4        |                      | 0.37      |                     |                   |
|             | BMAK-3 | -0.55                    | (-1.14) - 0.57                        | 1.3        | 0.2-5.4              | 0.07      | 0.04-2.29           | Middle intertidal |
|             | BMAK-2 | -0.05                    |                                       | 0.2        |                      | 0.04      |                     |                   |
|             | BMAK-1 | 0.42                     |                                       | 0.2        |                      | 0.05      |                     |                   |
|             | AMAK-1 | 0.57                     |                                       | 0.2        |                      | 0.09      |                     |                   |
|             | CMAK-3 | 1.01                     | 0.57-1.51                             | 0          | 0-0.2                | 0         | 0-0.04              | Higher intertidal |
|             | CMAK-1 | 1.48                     |                                       | 0          |                      | 0         |                     |                   |
| CMAK-2      | 1.51   | 0                        |                                       | 0          |                      |           |                     |                   |
| Unguja Ukuu | A-UU-3 | 0.01                     | 0.01-0.21                             | 2.23       | 0.17-2.23            | 0.59      | 0.20-0.59           | Lower intertidal  |
|             | A-UU-1 | 0.07                     |                                       | 0.88       |                      | 0.20      |                     |                   |
|             | B-UU-1 | 0.14                     |                                       | 0.72       |                      | 0.25      |                     |                   |
|             | A-UU-2 | 0.21                     |                                       | 0.17       |                      | 0.33      |                     |                   |
|             | B-UU-2 | 0.86                     | 0.21-1.91                             | 0.04       | 0-0.17               | 0.16      | 0-0.20              | Higher intertidal |
|             | B-UU-3 | 0.99                     |                                       | 0.04       |                      | 0.08      |                     |                   |
|             | C-UU-1 | 1.35                     |                                       | 0.02       |                      | 0.05      |                     |                   |
|             | C-UU-3 | 1.89                     |                                       | 0          |                      | 0         |                     |                   |
|             | C-UU-2 | 1.91                     |                                       | 0          |                      | 0         |                     |                   |

1152  
1153  
1154  
1155  
1156  
1157  
1158  
1159  
1160  
1161  
1162  
1163  
1164 392  
1165  
1166 393 Table 2. Vegetation plots of Makoba Bay and Unguja Ukuu showing  
1167  
1168 394 *Sonneratia/(Bruguiera/Ceriops)* (S/BC) and *Sonneratia/Rhizophora* (S/R) ratios  
1169  
1170 395 of surface samples developed from Punwong et al. (2013a; 2013b). The ranges of  
1171  
1172 396 ratios show the modern altitudinal range and are applied to infer the mangrove  
1173  
1174 397 position of sediment in core as modern analogue of lower intertidal, middle  
1175  
1176 398 intertidal, higher intertidal mangrove classes of the area with respect to altitude.

#### 1178 399 1179 1180 400 4.3. Chronology

1181  
1182  
1183 401 Nine radiocarbon dates were obtained from the northern Rufiji Delta  
1184  
1185 402 (Table 1). The radiocarbon dates indicate sedimentary hiatuses in the upper part of  
1186  
1187 403 BNR between 46 cm (4821- 4453 cal yr BP) and 19 cm (modern deposition) and  
1188  
1189 404 between 242 cm (799 - 680 cal yr BP) and 115 cm (modern deposition) in CNR.  
1190  
1191 405 The dates from 19 cm (BNR) and 115 cm (CNR) are therefore rejected for RSL  
1192  
1193 406 reconstruction. In ANR there is no pollen record between the depths of 115-150  
1194  
1195  
1196  
1197  
1198  
1199  
1200

1201  
1202  
1203  
1204 407 cm. The date from 128 cm of ANR is therefore not applicable for RSL  
1205  
1206 408 reconstruction.

1207  
1208 409 Eleven radiocarbon dates on bulk sediment were obtained from Makoba  
1209  
1210 410 Bay (Table 1). The radiocarbon dates from cores BMAK-1 (96 and 195 cm) and  
1211  
1212 411 CMAK-1 (107 and 172 cm) demonstrate age reversals. Despite their potential,  
1213  
1214 412 mangrove peats are notoriously difficult to date with age reversals common in  
1215  
1216 413 radiocarbon dated sequences, and modern ages often being reported from samples  
1217  
1218 414 collected several decimeters below the ground surface (e.g. Woodroffe and  
1219  
1220 415 Horton, 2005). The likely causes of these dating problems are reworking of  
1221  
1222 416 mangrove sediments through root penetration introducing younger carbon lower  
1223  
1224 417 down in the sediment profile and mixing of older sediments within the upper unit  
1225  
1226 418 (Punwong et al., 2013b; Woodroffe et al., 2015a). The nine dates obtained from  
1227  
1228 419 the organic concentrates reveal a coherent chronology and logical age-depth  
1229  
1230 420 relationship suggesting reliable dates for AMAK-1 and BMAK-1 (Woodroffe et  
1231  
1232 421 al., 2015a). It would therefore appear that the source of contamination, such as the  
1233  
1234 422 penetration of mangrove roots into the sediment matrix and bioturbation at depth,  
1235  
1236 423 taking younger carbon down the core (Punwong et al., 2013b; Woodroffe et al.,  
1237  
1238 424 2015a). We therefore reject the dates on bulk sediments from the cores AMAK-1,  
1239  
1240 425 BMAK-1 and the two reversed dates (at 107 and 172 cm) of CMAK-1 and use the  
1241  
1242 426 organic concentrate dates for RSL reconstruction. In CMAK-1, there is no pollen  
1243  
1244 427 record between the depths of 105-174 cm. The date from 130 cm of CMAK-1 is  
1245  
1246 428 therefore not used for RSL reconstruction.

1247  
1248  
1249 429 Six radiocarbon dates were obtained from Unguja Ukuu (Table 1). The  
1250  
1251 430 radiocarbon date from core C-UU-4 (42 cm) records modern age deposition,  
1252  
1253  
1254  
1255  
1256  
1257  
1258  
1259  
1260

1261  
1262  
1263  
1264 431 probably due to contamination (as described above) and this date is therefore  
1265  
1266 432 rejected for RSL reconstruction.

1267  
1268 433

#### 1269 434 4.4. RSL and compaction

1270  
1272 435 In order to reconstruct RSL changes using mangrove sediments, the upper  
1273  
1274 436 and lower limits of mangrove vegetation with reference to the mean tide level  
1275  
1276 437 (MTL) is used in order to establish an indicative range for mangroves following  
1277  
1278 438 the approach of Woodroffe et al. (2015b) and Hijma et al. (2015). The indicative  
1279  
1280 439 ranges for mangrove sediments are +2.57 m MTL  $\pm$  0.90 m in the northern Rufiji  
1281  
1282  
1283 440 Delta, -0.08 m MTL  $\pm$  1.55 m in Makoba Bay and +0.92 m MTL  $\pm$  0.95 m in  
1284  
1285 441 Unguja Ukuu (Table 1; Figure 2a). To reduce the vertical error, where detailed  
1286  
1287 442 contemporary vegetation pollen studies were undertaken in Makoba Bay and  
1288  
1289 443 Unguja Ukuu, we use the pollen ratios of S/BC and S/R to calculate the altitudinal  
1290  
1291 444 ranges of RSL (as described in 4.2 Pollen analysis and vegetation survey). For  
1292  
1293 445 example, the radiocarbon date of 1807-1548 cal yr BP occurs at the depth of 0.94  
1294  
1295 446 m in AMAK-1 from Makoba Bay; using the pollen ratios of S/BC and S/R  
1296  
1297 447 derived from contemporary pollen studies, it is possible that the vegetation at the  
1298  
1299 448 depth of 0.94 m represent a middle-intertidal mangrove association (Figure 2b). If  
1300  
1301 449 this is related to MTL using the vegetation plot data, the vertical error of the date  
1302  
1303 450 becomes  $\pm$  0.86 m derived from the vertical range of the middle-intertidal  
1304  
1305 451 mangrove that is -1.14 m MTL and +0.57 m MTL (Table 1 and 2). The indicative  
1306  
1307 452 range derived from the upper and lower limit of mangrove vegetation in Makoba  
1308  
1309 453 Bay is -0.08 m MTL and therefore the indicative range of RSL from the date is -  
1310  
1311 454 0.08 m MTL  $\pm$  0.86 m (Table 1).

1321  
1322  
1323  
1324 455 Sediments are susceptible to post-depositional compaction (Bird et al.,  
1325  
1326 456 2004; Horton and Shennan, 2009). A compaction factor for the mangrove  
1327  
1328 457 sediment was estimated by comparing the dry bulk density of a compacted sample  
1329  
1330 458 with the modern sediment sample and found to range from 17-31% (Bird et al.,  
1331  
1332 459 2004). As this geotechnical technique is beyond the scope of study, the worst-case  
1333  
1334 460 compaction scenario of Bird et al. (2004) of 31% was adopted for the  
1335  
1336 461 decompaction correction below the depth dated (Table 1). For example, at the  
1337  
1338 462 depth 1.07 m of BNR that is 4.50 m in total length, the compaction of mangrove  
1339  
1340 463 sediment below this depth would be 1.0633 m (31% of 4.50 – 1.07 m) and would  
1341  
1342 464 be applied to the vertical error in an upward direction. This approach has also  
1343  
1344 465 been used in mangrove sea-level reconstructions from mangrove deposits in the  
1345  
1346 466 Seychelles (Woodroffe et al., 2015b).

1347  
1348  
1349 467 Vertical errors also include compaction caused by the coring equipment ( $\pm$   
1350  
1351 468 0.04 m) (Woodroffe, 2006), levelling errors ( $\pm$  0.051 m), and the vertical range of  
1352  
1353 469 the radiocarbon date ( $\pm$  0.005 m). Sea-level tendency for each RSL reconstruction  
1354  
1355 470 is determined (Table 1) by using a combination of stratigraphy and the trend of  
1356  
1357 471 mangrove pollen-based interpretation from each coring site (Figure 2b).

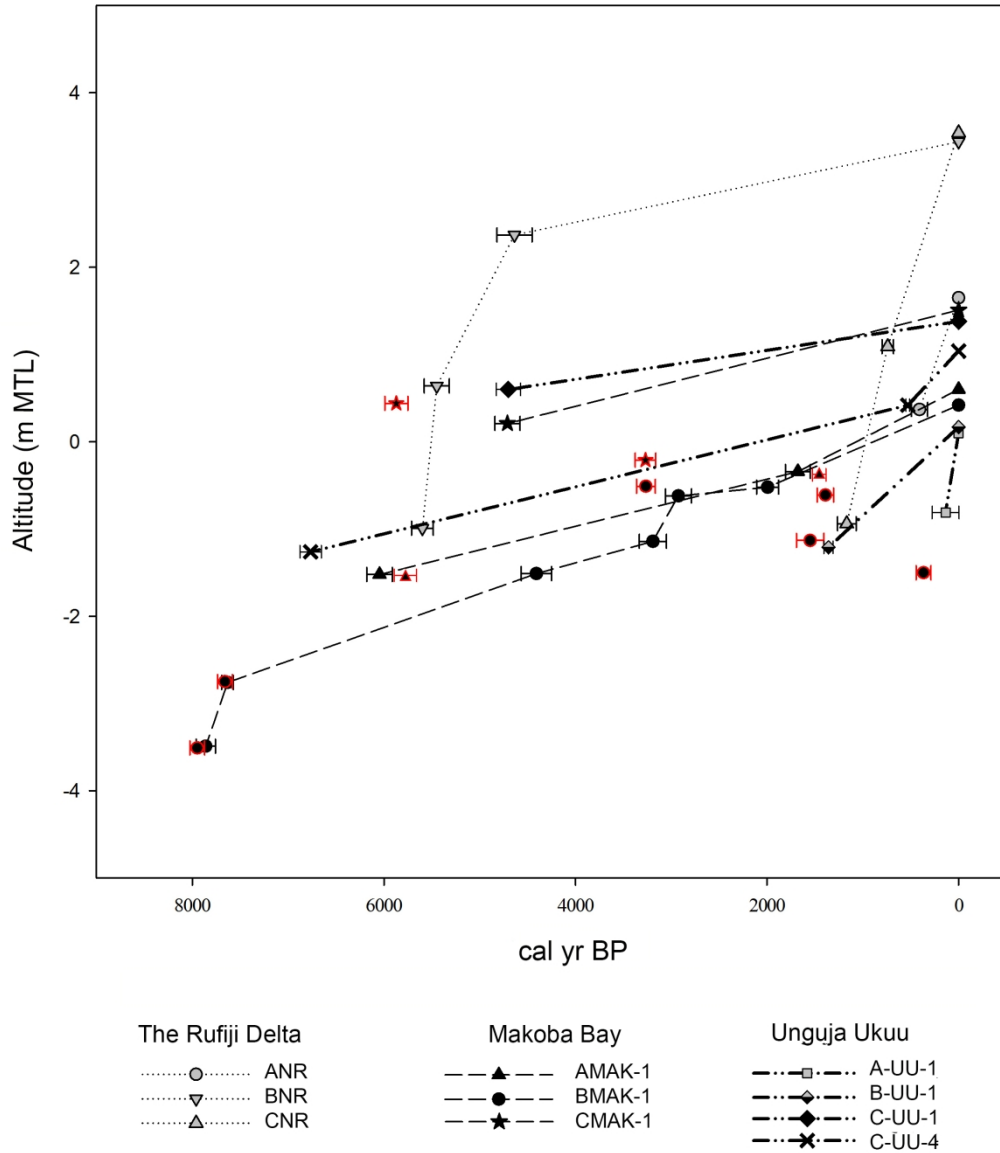
1358  
1359  
1360 472

## 1361 1362 473 5. Interpretation and discussion

1363  
1364 474 Age-depth plots of the cores indicated that the basal age for each core  
1365  
1366 475 ranged from ~ 7900 cal yr BP (BMAK-1 of Makoba Bay) to ~100 cal yr BP (A-  
1367  
1368 476 UU-1 of Unguja Ukuu). A comparison of sedimentation rates showed great  
1369  
1370 477 variation between the Rufiji Delta and Zanzibar sites (Figure 3). Although the  
1371  
1372 478 chronology is problematic, it would appear that the sedimentation rate of between  
1373  
1374 479 2.1-10.9 mm cal yr<sup>-1</sup> for the Rufiji Delta was considerably higher than that for  
1375  
1376  
1377  
1378  
1379  
1380



1381  
1382  
1383  
1384 480 Makoba Bay and Unguja Ukuu (0.3-6.6 mm cal yr<sup>-1</sup>). This enhanced  
1385  
1386 481 sedimentation rate is probably due to the nature of the deltaic mangrove setting  
1387  
1388 482 with river discharge transporting sediment from the wider Rufiji catchment to be  
1389  
1390 483 deposited into the Rufiji Delta (Semesi, 1992; Fisher et al., 1994). The variation in  
1391  
1392 484 sedimentation rates results in different altitudinal ranges of the mangrove areas at  
1393  
1394 485 the three locations with freshwater input, sediment supply and progradation  
1395  
1396 486 having significantly more effect in the Rufiji Delta than at the Zanzibar sites.  
1397  
1398 487 However, given site-specific responses of mangroves relative to sea level, when  
1399  
1400 488 sites are combined, they provide regional RSL reconstruction.  
1401  
1402  
1403 489  
1404  
1405  
1406  
1407  
1408  
1409  
1410  
1411  
1412  
1413  
1414  
1415  
1416  
1417  
1418  
1419  
1420  
1421  
1422  
1423  
1424  
1425  
1426  
1427  
1428  
1429  
1430  
1431  
1432  
1433  
1434  
1435  
1436  
1437  
1438  
1439  
1440



490

491 Figure 3. Comparative age-depth plots including rejected dates (in red edge) for  
 492 the cores analysed in this study. Comparative age-depth (altitude) models for the  
 493 cores analysed in this study. The top value against the zero origin (cal yr BP) on  
 494 all such graphs except BMAK-1 does not necessarily represent present day  
 495 deposition because of potential surface erosion.

496

497 5.1. Holocene mangrove dynamics

1441  
 1442  
 1443  
 1444  
 1445  
 1446  
 1447  
 1448  
 1449  
 1450  
 1451  
 1452  
 1453  
 1454  
 1455  
 1456  
 1457  
 1458  
 1459  
 1460  
 1461  
 1462  
 1463  
 1464  
 1465  
 1466  
 1467  
 1468  
 1469  
 1470  
 1471  
 1472  
 1473  
 1474  
 1475  
 1476  
 1477  
 1478  
 1479  
 1480  
 1481  
 1482  
 1483  
 1484  
 1485  
 1486  
 1487  
 1488  
 1489  
 1490  
 1491  
 1492  
 1493  
 1494  
 1495  
 1496  
 1497  
 1498  
 1499  
 1500

1501  
1502  
1503  
1504 498 Combined palaeoecological records from the three locations provide a new  
1505  
1506 499 palaeoenvironmental sea-level synthesis from Tanzania where relatively little is  
1507  
1508 500 known about the Holocene mangrove dynamics. The records reveal that mangrove  
1509  
1510 501 ecosystems have not remained stable as they responded to wide scale  
1511  
1512 502 environmental changes and there are some site-specific responses to  
1513  
1514 503 environmental shifts. The results further our understanding of how mangrove  
1515  
1516 504 ecosystems reflect environmental variables, and shifts in these, that could help  
1517  
1518 505 assess resilience of coastal ecosystems under future climatic scenarios,  
1519  
1520 506 particularly sea-level rise (Ellison, 2015).

1522  
1523 507 Early to mid Holocene

1525 508 The pollen record of BMAK-1 indicates that mangroves have been present  
1526  
1527 509 at Makoba Bay at -3.6 m below MTL since at least ~7900 cal yr BP (Figure 2b).  
1528  
1529 510 The ratios of S/BC and S/R suggest that the central core (BMAK-1) location was  
1530  
1531 511 colonised by higher intertidal mangroves (Figures 1f, 2b; Table 2) suggesting an  
1532  
1533 512 early Holocene RSL rise. A higher RSL rise was then recorded after this period  
1534  
1535 513 for a relatively short duration until ~7600 cal yr BP, as mangroves migrated  
1536  
1537 514 landward and this area supported middle intertidal mangrove taxa. RSL continued  
1538  
1539 515 to rise, as indicated by the ratios of mangrove pollen and the deposition of oyster  
1540  
1541 516 shells in BMAK-1b and AMAK-1. This marine transgression caused the  
1542  
1543 517 mangrove taxa at these two coring locations to migrate further landwards and  
1544  
1545 518 allowed mangroves to establish on the headland of Unguja Ukuu at -1.3 m MTL  
1546  
1547 519 as recorded ~6800 cal yr BP in C-UU-4. After this time, higher intertidal  
1548  
1549 520 mangroves recorded in C-UU-4 were replaced by lower intertidal mangrove taxa;  
1550  
1551 521 thus contributing to a body of evidence indicating that RSL continued to rise  
1552  
1553 522 during the mid Holocene (Camoin et al., 1997; 2004; Zinke et al., 2003; Norström  
1554  
1555  
1556  
1557  
1558  
1559  
1560

1561  
1562  
1563  
1564 523 et al., 2012). It should be noted that the pollen records from both sites in Zanzibar  
1565  
1566 524 reveals a similar age determination of 5600 cal yr BP and a similar pollen record,  
1567  
1568 525 lending support to the chronological and sea-level interpretation from BNR in the  
1569  
1570 526 northern Rufiji Delta (Punwong et al., 2012). The predominance of *R. mucronata*  
1571  
1572 527 pollen suggests that BNR was located in a low intertidal environment, a further  
1573  
1574 528 indication of a higher sea level relative to the present day. A mid Holocene RSL  
1575  
1576 529 rise possibly attained a higher altitude after 4700 cal yr BP resulting in higher  
1577  
1578 530 intertidal mangroves establishment at 0.5 m above MTL in CMAK-1 and higher  
1579  
1580 531 intertidal mangrove establishment at 0.6 m MTL in C-UU-1. This mid Holocene  
1581  
1582 532 RSL rise occurred until prior to ~4400 cal yr BP, when RSL started to fall as  
1583  
1584 533 indicated by the transition from lower intertidal to middle intertidal mangroves in  
1585  
1586 534 BMAK-1.

1587  
1588  
1589 535  
1590  
1591 536 Mid Holocene to the present day

1592  
1593 537 After ~4400 cal yr BP mangrove ecosystem character varied between the  
1594  
1595 538 sites reflecting different RSL changes. A lower RSL is recorded in Makoba Bay  
1596  
1597 539 from ~4400 cal yr BP, as indicated by the change in mangrove composition from  
1598  
1599 540 lower to middle intertidal mangroves in BMAK-1 until ~3200 cal yr BP. This  
1600  
1601 541 period coincides with a regionally arid phase recorded across East Africa  
1602  
1603 542 commencing around 4500–4100 cal yr BP (Hassan, 1997; Bonnefille and Chalieu,  
1604  
1605 543 2000; Thompson et al., 2002; Marchant and Hooghiemstra, 2004; Kiage and Liu,  
1606  
1607 544 2006; Rijdsdijk et al., 2011; de Boer et al., 2015). After 3200 cal yr BP, and prior  
1608  
1609 545 to 2900 cal yr BP, a RSL rise occurred indicative of a change from middle to  
1610  
1611 546 lower intertidal mangroves. Mangrove composition subsequently changed to  
1612  
1613 547 middle intertidal mangroves in AMAK-1 and BMAK-1 (Figure 2b) suggesting a  
1614  
1615  
1616  
1617  
1618  
1619  
1620

1621  
1622  
1623  
1624 548 lower RSL as mangroves retreated seaward until the late Holocene ~2000-1700  
1625  
1626 549 cal yr BP. However, a sea-level rise is recorded at Unguja Ukuu as lower  
1627  
1628 550 intertidal mangroves occupied C-UU-1 and C-UU-4 after the mid Holocene until  
1629  
1630 551 ~500 cal yr BP. The apparent discrepancy in RSL between these two sites at  
1631  
1632 552 Unguja after 4400 to 1700 cal yr BP is probably due to local processes including  
1633  
1634 553 mangrove composition response to sediment input and/or erosion at the sites,  
1635  
1636 554 resulting in localised RSL changes.

1638  
1639 555 The late Holocene RSL fall is recorded at all three sites. In Makoba Bay,  
1640  
1641 556 RSL fell until the present day, as suggested by the change of middle intertidal  
1642  
1643 557 mangroves to higher intertidal mangroves in AMAK-1 and BMAK-1. At Unguja  
1644  
1645 558 Ukuu, lower intertidal mangroves changed to higher intertidal mangroves after  
1646  
1647 559 1400 cal yr BP in B-UU-1. RSL probably continued falling in Unguja Ukuu, as  
1648  
1649 560 represented by the change from lower intertidal mangroves to higher intertidal  
1650  
1651 561 mangroves after ~500 cal yr BP in C-UU-4, and the presence of more intertidal  
1652  
1653 562 mangroves after ~100 cal yr BP in A-UU-1. In the Rufiji Delta, a reduction in  
1654  
1655 563 mangrove pollen and increase in back-mangrove and terrestrial grasses in the  
1656  
1657 564 landward site (CNR) after 1200 cal yr BP resulted in a shift of mangroves  
1658  
1659 565 seaward. RSL then fluctuated, as suggested by changes in the proportions of  
1660  
1661 566 mangroves, back-mangrove and terrestrial grasses until prior to 700 cal yr BP.  
1662  
1663 567 After 700 cal yr BP, RSL started to fall, as recorded by a gradual change from  
1664  
1665 568 mangroves characterised by *R. mucronata* to terrestrial vegetation, and a  
1666  
1667 569 replacement of mangroves by recent herbaceous taxa. However, changes from  
1668  
1669 570 higher intertidal mangroves to lower intertidal mangroves in A-UU-1, B-UU-1  
1670  
1671 571 and C-UU4 at Unguja Ukuu, corresponding to an increase in *A. marina* at the top  
1672  
1673  
1674  
1675  
1676  
1677  
1678  
1679  
1680

1681  
1682  
1683  
1684 572 of ANR, are likely to represent a signal of sea-level rise during the last few  
1685  
1686 573 hundred years.

1687  
1688 574

1689  
1690 575 5.2. Sea-level reconstruction

1691  
1692 576 The pollen evidence from the Rufiji Delta, Makoba Bay and Unguja Ukuu  
1693  
1694 577 can be used to reconstruct the Holocene RSL from Tanzania using the upper and  
1695  
1696 578 lower limits of mangrove vegetation and shift in recognisable salinity tolerance  
1697  
1698 579 zones of the mangrove ecosystem. The RSL derived from the pollen ratios within  
1699  
1700 580 the vegetation plots can refine vertical errors (Figure 4). Regardless of site-  
1701  
1702 581 specific characteristics, it should be noted that all three sites provide evidence for  
1703  
1704 582 a phase of early-mid Holocene RSL rise and late Holocene RSL fluctuation. The  
1705  
1706 583 composite RSL curve shows that RSL rise occurred from around 7900 cal yr BP.  
1707  
1708 584 It is possible that RSL rose and was potentially higher than present at ~4700-4600  
1709  
1710 585 cal yr BP. However, when the sites are compared (Figure 4), variations in the rate  
1711  
1712 586 of sea level rise are noted. In the northern Rufiji Delta, the higher sedimentation  
1713  
1714 587 rates are probably due to the large freshwater and terrestrial inputs to the system.

1715  
1716  
1717 588 The general trend of the early to mid Holocene RSL rise (Figure 4)  
1718  
1719 589 appears to be in agreement with RSL trends from other locations such as the  
1720  
1721 590 mainland coast and offshore islands in the Southwest Indian Ocean (Colonna et  
1722  
1723 591 al., 1996; Camoin et al., 1997; 2004; Zinke et al., 2000; Compton, 2001; Ramsay  
1724  
1725 592 and Cooper, 2002; Zinke et al., 2003).

1726  
1727  
1728 593 The proposed higher than present sea level at around 4700-4600 cal yr BP  
1729  
1730 594 recorded in Tanzania indicates a similar trend to that recorded from South Africa  
1731  
1732 595 (Compton, 2001; Ramsay and Cooper, 2002) (Figure 4). The mid Holocene RSL  
1733  
1734 596 rise in Tanzania is also comparable to a marine transgression phase in  
1735  
1736  
1737  
1738  
1739  
1740

1741  
1742  
1743  
1744 597 Mozambique (Norström et al., 2012) where a highstand is recorded ~6600-6300  
1745  
1746 598 cal yr BP. The mid Holocene transgression is well represented from the Southern  
1747  
1748 599 Hemisphere in far-field locations (Isla, 1989) relating to three possible causes  
1749  
1750 600 including meltwater from late glacial ice sheets (Lambeck and Nakada, 1990;  
1751  
1752 601 Fleming et al., 1998) and/or the Holocene melting of ice sheets from Antarctica,  
1753  
1754 602 Greenland and mountain glaciers during the early Holocene until 5000 cal yr BP  
1755  
1756 603 (Milne et al., 2005).

1758  
1759 604 Evidence from Mauritius, Mayotte and Réunion Island (Camoin et al.,  
1760  
1761 605 1997; 2004; Zinke et al., 2003) suggest no mid Holocene highstand occurred at  
1762  
1763 606 these locations. The differences between the records from the islands and  
1764  
1765 607 Tanzania may result from hydro-isostatic influences relating to the differences in  
1766  
1767 608 the geographical locations of the Tanzanian coast and the islands (Clark et al.,  
1768  
1769 609 1978). The Holocene highstand at small offshore islands is likely to be less  
1770  
1771 610 marked than at the continental margins due to the effects of continental levering  
1772  
1773 611 (Lambeck and Nakada, 1990; Mitrovica and Milne, 2002; Milne and Mitrovica,  
1774  
1775 612 2008). However, the highstand recorded from South Africa is likely to be higher  
1776  
1777 613 than the potential maximum transgression at ~4700 cal yr BP and 4600 cal yr BP  
1778  
1779 614 in Tanzania (Compton, 2001; Ramsay and Cooper, 2002). In addition to eustatic  
1780  
1781 615 changes, a combination of various factors such as hydro-isostasy, thermal  
1782  
1783 616 expansion of sea water caused by warmer ocean temperatures in subtropical  
1784  
1785 617 latitudes (Ramsay, 1995, Woodroffe and Horton, 2005), and the steric expansion  
1786  
1787 618 of sea water (Ramsay, 1995; Compton, 2001) may also be considered as factors  
1788  
1789 619 enhancing the highstand altitude in South Africa.

1792  
1793 620 RSL fell from 4600 cal yr BP to 4400 cal yr BP. After 4400 cal yr BP,  
1794  
1795 621 RSL slightly rose until ~2000 cal yr BP. The RSL record at this time from  
1796  
1797  
1798  
1799  
1800

1801  
1802  
1803  
1804 622 Tanzania correlates well with records from South Africa (Ramsay and Cooper,  
1805  
1806 623 2002) and also corresponds with a possible marine transgression with a highstand  
1807  
1808 624 from Macassa Bay (Mozambique) between 4000 - 1100 cal yr BP (Norström et  
1809  
1810 625 al., 2012). The pollen records from Makoba Bay and C-UU-1 and C-UU-4 of  
1811  
1812 626 Unguja Ukuu indicate that mangrove development continued after the mid  
1813  
1814 627 Holocene RSL rise indicating a sustained higher level that did not fall until the  
1815  
1816 628 late Holocene ~2000 cal yr BP. This may have allowed suitable conditions for  
1817  
1818 629 mangroves to establish at A-UU-1 and B-UU-1 and may correspond to the  
1819  
1820 630 progradation of beach plains that is recorded in Zanzibar (Arthurton, 2003).

1821  
1822  
1823 631 The late Holocene RSL record after 2000 cal yr BP until 100 cal yr BP  
1824  
1825 632 correlates well with the RSL records from South Africa (Compton, 2001; Ramsay  
1826  
1827 633 and Cooper, 2002) and Mozambique (Norström et al., 2012) (Figure 4). A lower  
1828  
1829 634 sea level occurred in Tanzania until 1400 - 1200 cal yr BP; this RSL fall is also  
1830  
1831 635 recorded in northeastern South Africa ~1400 cal yr BP to the present (Ramsay and  
1832  
1833 636 Cooper, 2002). We acknowledged that potential sea-level fall would correspond to  
1834  
1835 637 climatically cold phases and sea-level rise to warm phases, as a result of the  
1836  
1837 638 glacial eustasy (Oerlemans, 2001). Changes in rainfall can also cause local  
1838  
1839 639 eustatic sea-level changes (Mörner, 1996). However, easternmost East Africa  
1840  
1841 640 experienced drought during the Medieval Warm Period (MWP) (900 - 700 cal yr  
1842  
1843 641 BP) and wet conditions during the Little Ice Age (LIA) (700 - 100 cal yr BP)  
1844  
1845 642 (Verchuren et al., 2000). These phases are contrast with our records of sea-level  
1846  
1847 643 transgression after 1200 - 500 cal yr BP and sea-level regression from 500 - 100  
1848  
1849 644 cal yr BP. Archaeological sites in Unguja Ukuu indicate that RSL was  
1850  
1851 645 approximately -0.5 m below the present level between ~1300 - 1000 cal yr BP  
1852  
1853 646 (Mörner, 1992). This is in good agreement with the reconstruction from the three  
1854  
1855  
1856  
1857  
1858  
1859  
1860

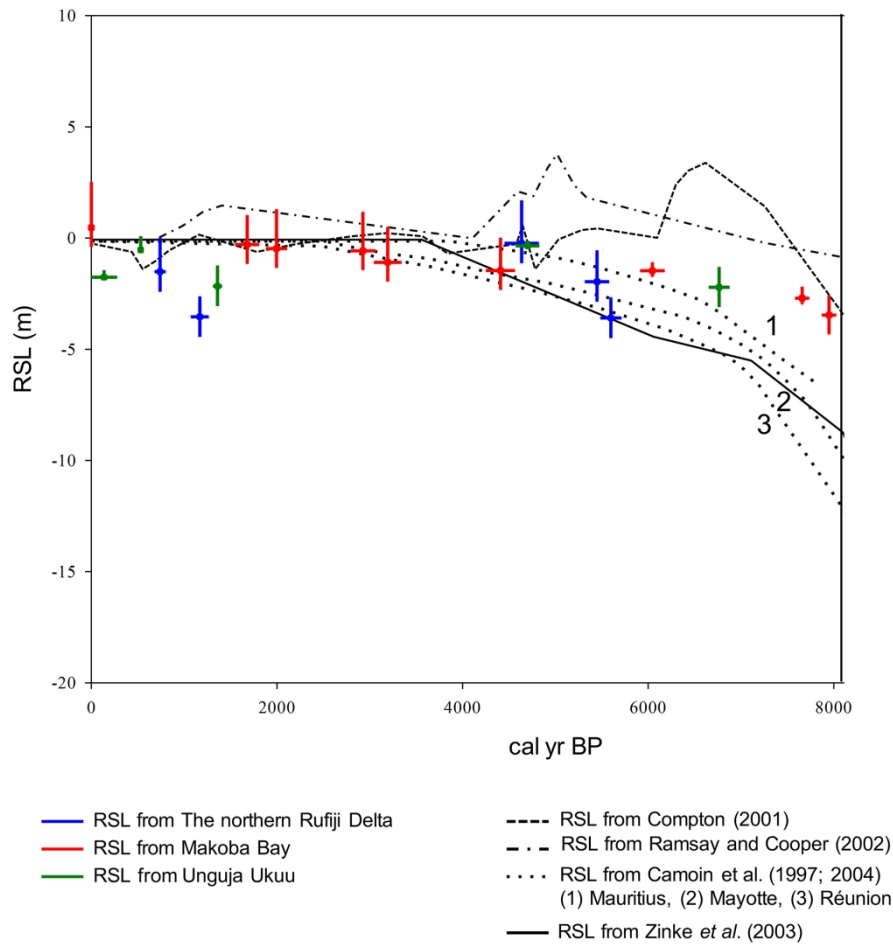


1861  
1862  
1863  
1864 647 sites studied suggesting RSL did not attain present sea level between 1400-1200  
1865  
1866 648 cal yr BP (Figure 4).

1868 649 A further RSL rise occurred after 1200 to ~700 - 500 cal yr BP and it is  
1869  
1870 650 likely that RSL was below the present sea level. This concurs with records from  
1871  
1872 651 ruins in southeastern Tanzania (Kilwa) suggesting RSL was about -1 m below the  
1873  
1874 652 present level between 800- 600 cal yr BP (Mörner, 1992). After this period, RSL  
1875  
1876 653 fell until ~100 cal yr BP when sea level was lower than the present day. This is in  
1877  
1878 654 good agreement with a study of raised terraces along the Kenyan coast indicating  
1879  
1880 655 that RSL started to fall 500 years ago (Åse, 1978; 1981). In contrast, data from  
1881  
1882 656 Mozambique (Norström et al., 2012) and southern Langebaan Lagoon in South  
1883  
1884 657 Africa (Compton, 2001) show somewhat conflicting results from the Tanzanian  
1885  
1886 658 data indicating RSL fell after 1200 cal yr BP. After 100 cal yr BP, RSL rose until  
1887  
1888 659 the present day corresponding to the onset of recent sea-level rise from the 19<sup>th</sup>  
1889  
1890 660 century (Stocker et al., 2013) as recorded in Kenya between 1986-2002 (Kibue,  
1891  
1892 661 2006). However, a recent sea-level fall was observed in Zanzibar between 1985-  
1893  
1894 662 2001 (Permanent Service for Mean Sea Level) before rising trend was observed to  
1895  
1896 663 the present day. In addition, it should be noted that Makoba and Unguja Ukuu  
1897  
1898 664 which all are on the west cost of Unguja Island and separated by 40 km shows  
1899  
1900 665 different RSL especially during the last 2000 years probably due to local  
1901  
1902 666 processes, such as changes in sediment input and/or erosion at the sites.

1906 667 Difficulties encountered in dating suggest additional records and  
1907  
1908 668 chronological control using dating of pollen concentrates is required to determine  
1909  
1910 669 a high-resolution record of mid Holocene sea level and environmental changes.  
1911  
1912 670 Although the evidence from Tanzania demonstrates the site-specific nature of  
1913  
1914 671 responses of mangroves to RSL changes, it does provide a valuable contribution  
1915  
1916  
1917  
1918  
1919  
1920

1921  
 1922  
 1923  
 1924 672 to patterns of Holocene RSL from “far-field” locations. There is great potential to  
 1925  
 1926 673 scale up the type of investigation presented here to other coastal mangrove sites  
 1927  
 1928 674 across East Africa, as well as offshore islands. Such an extension to this study  
 1929  
 1930 675 would provide an unprecedented regional record of environmental and sea-level  
 1931  
 1932 676 changes from a far-field region and allow us to distinguish large and meso-scale  
 1933  
 1934  
 1935 677 regional signals against site-specific responses across East Africa.



678  
 679 Figure 4. RSL reconstructions from this study along the Tanzanian coast plotted  
 680 alongside RSL curves from the southwest Indian Ocean region

681  
 682 6. Conclusions

1981  
1982  
1983  
1984 683 A reconstruction of Holocene RSL has been derived for coastal Tanzania  
1985  
1986 684 from mangrove ecosystem changes from three sites. The ratios of  
1987  
1988 685 *Sonneratia:(Bruguiera/Ceriops)* and *Sonneratia:Rhizophora* derived from the  
1989  
1990 686 pollen-vegetation-altitude relationships can be used to interpret mangrove  
1991  
1992 687 dynamics and refine the vertical errors of RSL changes derived from mangrove  
1993  
1994 688 sediments. Although the results in part demonstrate the site-specific shifts in the  
1995  
1996 689 upper and lower limits of mangroves relative to sea level, due to responses of  
1997  
1998 690 sediment input and/or erosion at the three sites, they do provide evidence for  
1999  
2000 691 Holocene RSL fluctuations coherent across coastal Tanzania. An early-mid to mid  
2001  
2002 692 Holocene RSL rise occurred from ~ 7900 cal yr BP prior to ~4700-4600 cal yr BP  
2003  
2004 693 when RSL was potentially higher than the present. This period is followed by a  
2005  
2006 694 lower RSL until 4400 cal yr BP when RSL rose until ~2000 cal yr BP.  
2007  
2008 695 Subsequently, late Holocene RSL fluctuations were characterised by RSL rise  
2009  
2010 696 recorded at ~700 - 500 cal yr BP before falling below the present level at ~100 cal  
2011  
2012 697 yr BP. There is evidence of a more recent RSL rise during the last centuries. The  
2013  
2014 698 Tanzanian RSL curve indicates a similar trend to the mid Holocene RSL record  
2015  
2016 699 from South Africa, probably related to similar hydro-isostatic conditions  
2017  
2018 700 representing the apparent Holocene highstand at continental margins due to the  
2019  
2020 701 effects of continental levering. The RSL fall recorded during the last 500 years is  
2021  
2022 702 in good agreement with the records from the Kenyan coast, although data from  
2023  
2024 703 Mozambique and the Langebaan Lagoon in South Africa indicate RSL fell after  
2025  
2026 704 1200 cal yr BP. The difficulties of developing a reliable chronology from  
2027  
2028 705 mangrove environments have previously precluded extensive use of these  
2029  
2030 706 sediment archives for reconstructing RSL changes. Organic concentrate dating  
2031  
2032 707 applied on some of the samples presented here can provide a reliable chronology  
2033  
2034  
2035  
2036  
2037  
2038  
2039  
2040

2041  
2042  
2043  
2044 708 allowing these far-field locations to be fully investigated and used as a proxy for  
2045  
2046 709 reconstructing eustatic sea-level changes. Site-specific signals of RSL change,  
2047  
2048 710 mangrove response to this and the need to further constrain the pollen-vegetation-  
2049  
2050 711 environmental relationships all emphasise the need for further research along the  
2051  
2052 712 East African coast, as well as other “far-field” locations, so that the full potential  
2053  
2054 713 of the mangrove sedimentary sea-level archive can be fully realised.  
2055

2056  
2057 714

## 2058 715 Acknowledgements

2059  
2060 716 This work was carried out as a part of doctoral thesis at the University of  
2061  
2062 717 York. Thanks are extended to Mr William Kindeketa and Rebecca Newman for  
2063  
2064 718 their support and assistance throughout the fieldwork. We would like to thank the  
2065  
2066 719 Palynology & Palaeobotany Section, National Museums of Kenya for lending us  
2067  
2068 720 the coring equipment necessary for fieldwork and laboratory work, WWF-  
2069  
2070 721 Tanzania for providing logistical support for the fieldwork in Rufiji Delta and Mr  
2071  
2072 722 Benson Kimeu, Survey/GIS Technician from The British Institute in Eastern  
2073  
2074 723 Africa for conducting the elevation survey. I am grateful to Professor Antony  
2075  
2076 724 Long, Dr. Sarah Woodroffe and Dr. Sanpisa Sritrairat for their constructive  
2077  
2078 725 comments on earlier versions of this manuscript. The radiocarbon dates on the  
2079  
2080 726 organic concentrates was funded through NERC Radiocarbon Facility Allocation  
2081  
2082 727 1608.0312. This study was supported by The Royal Thai Government Scholarship  
2083  
2084 728 and the Development and Promotion Science and Technology Talents project.  
2085  
2086 729

2087  
2088 729

## 2089 730 References

2090  
2091  
2092 731  
2093  
2094  
2095  
2096  
2097  
2098  
2099  
2100

2101  
2102  
2103  
2104  
2105  
2106  
2107  
2108  
2109  
2110  
2111  
2112  
2113  
2114  
2115  
2116  
2117  
2118  
2119  
2120  
2121  
2122  
2123  
2124  
2125  
2126  
2127  
2128  
2129  
2130  
2131  
2132  
2133  
2134  
2135  
2136  
2137  
2138  
2139  
2140  
2141  
2142  
2143  
2144  
2145  
2146  
2147  
2148  
2149  
2150  
2151  
2152  
2153  
2154  
2155  
2156  
2157  
2158  
2159  
2160

732 Admiralty Tide Tables, 2014. NP203 Admiralty Tide Tables (ATT) Volume 3,  
733 Indian Ocean and South China Sea (including Tidal Stream Tables).  
734 Hydrographer to the Navy. Admiralty Hydrography Department. 365 pp.  
735 Arthurton, R.S., Brampton, A.H., Kaaya, C.Z., Mohamed, S.K., 1999. Late  
736 Quaternary coastal stratigraphy on a platform-fringed tropical coast- a case study  
737 from Zanzibar, Tanzania. *Journal of Coastal Research* 15, 635-644.  
738 Arthurton, R., 2003. The fringing reef coasts of eastern Africa-present processes  
739 in their long-term context. *Western Indian Ocean Journal Marine Science* 2 (1), 1-  
740 13.  
741 Åse, L.E., 1978. Preliminary Report on Studies of Shore Displacement at the  
742 Southern Coast of Kenya. *Geografiska Annaler, Series A, Physical Geography*,  
743 60, 3/4, 209-221.  
744 Åse, L.E., 1981. Studies of Shores and Shore Displacement on the Southern Coast  
745 of Kenya. Especially in the Kilifi District. *Geografiska Annaler, Series A*,  
746 *Physical Geography*, 63, 3/4, 303-310.  
747 Baker, R.G., Haworth, R., Flood, P., 2001. Inter-tidal fixed indicators of former  
748 Holocene sea levels in Australia: a summary of sites and a review of methods and  
749 models. *Quaternary International* 83–85, 257–273.  
750 Banerjee, P.K., 2000. Holocene and Late Pleistocene relative sea level  
751 fluctuations along the east coast of India. *Marine Geology* 167, 243–260.  
752 Bird, M. I., L. K. Fifield, S. Chua, Goh, B., 2004. Calculating sediment  
753 compaction for radiocarbon dating of intertidal sediments. *Radiocarbon* 46(1),  
754 421–435.

- 2161  
2162  
2163  
2164 755 Bird, M.I., Fifield, L.K., Teh, T.S., Chang, C.H., Shirlaw, N., Lambeck, K., 2007.  
2165  
2166 756 An inflection in the rate of early-mid Holocene eustatic sea-level rise: A new sea-  
2167  
2168 757 level curve from Singapore. *Estuarine, Coastal and Shelf Science* 71, 523–536.  
2169  
2170 758 Blasco, F., Saenger, P., Janodet, E. 1996. Mangroves as indicators of coastal  
2171  
2172 759 change. *Catena* 27, 167–178.  
2173  
2174 760 Bonnefille, R., Chalieu, F., 2000. Pollen-inferred precipitation time-series from  
2175  
2176 761 equatorial mountains, Africa, the last 40 kyr BP. *Global Planet Change* 26, 25–50.  
2177  
2178 762 Bronk-Ramsey, C., 2009. OxCal Program v4.10. Oxford Radiocarbon Accelerator  
2179  
2180 763 Unit, Oxford.  
2181  
2182 764 Camoin, G.F., Colonna, M., Montaggioni, L.F., Casanova, J., Faure, G.,  
2183  
2184 765 Thomassin, B.A., 1997. Holocene sea level changes and reef development in the  
2185  
2186 766 southwestern Indian Ocean. *Coral Reefs* 16 (4), 247–259.  
2187  
2188 767 Camoin, G.F., Montaggioni, L.F., Braithwaite, C.J.R., 2004. Late glacial to post  
2189  
2190 768 glacial sea levels in the Western Indian Ocean. *Marine Geology* 206, 119–146.  
2191  
2192 769 Clark, J.A., Farrell, W.E., Peltier, W.R., 1978. Global changes in post glacial sea  
2193  
2194 770 level: a numerical calculation. *Quaternary Research* 9, 265–287.  
2195  
2196 771 Cohen, M.C.L., Behling, H., Lara, R.J., 2005. Amazonian mangrove dynamics  
2197  
2198 772 during the last millennium: The relative sea-level and the Little Ice Age. *Review*  
2199  
2200 773 *of Palaeobotany and Palynology* 136, 93-108.  
2201  
2202 774 Colonna, M., Casanova, J., Dullo, W.C., Camoin, G., 1997. Sea-level changes and  
2203  
2204 775  $\delta^{18}\text{O}$  record for the past 34,000 yr from Mayotte Reef, Indian Ocean.  
2205  
2206 776 *Oceanographic Literature Review* 44(7), 693–693.  
2207  
2208 777 Compton, J.S., 2001. Holocene sea-level fluctuations inferred from the evolution  
2209  
2210 778 of depositional environments of the southern Langebaan Lagoon salt marsh, South  
2211  
2212 779 Africa. *The Holocene* 11(4), 395–405.  
2213  
2214  
2215  
2216  
2217  
2218  
2219  
2220

- 2221  
2222  
2223  
2224 780 Davis, O.K., 1984. Pollen frequencies reflect vegetation patterns in a Great Basin  
2225  
2226 781 (U.S.A.) mountain range. *Review of Palaeobotany and Palynology* 40, 295–315.  
2227  
2228 782 de Boer, E.J., Véléz, M.I., Rijdsdijk, K.F., de Louw, P.G., Vernimmen, T.J., Visser,  
2229  
2230 783 P.M., Tjallingii, R. and Hooghiemstra, H., 2015. A deadly cocktail: How a  
2231  
2232 784 drought around 4200 cal. yr BP caused mass mortality events at the infamous  
2233  
2234 785 ‘dodo swamp’ in Mauritius. *The Holocene*, 25(5), 758–771.  
2235  
2236 786 Ellison, A.M., Farnsworth, E.J., 2001. Mangrove communities. In: Bertness,  
2237  
2238 787 M.D., Gaines, S.D., Hay, M.E. (Eds.). *Marine Community Ecology*. Sinauer  
2239  
2240 788 Associates, Sunderland, MA. pp. 423–442.  
2241  
2242  
2243 789 Ellison, J.C., 1989. Pollen analysis of mangrove sediments as a sea level  
2244  
2245 790 indicator: assessment from Tongatapu, Tonga. *Palaeogeography,*  
2246  
2247 791 *Palaeoclimatology, Palaeoecology* 74: 327–341.  
2248  
2249 792 Ellison, J.C., 2005. Holocene palynology and sea-level change in two estuaries in  
2250  
2251 793 Southern Irian Jaya. *Palaeogeography and Palaeoclimatology*. 220, 291–309.  
2252  
2253 794 Ellison, J.C., 2008. Long-term retrospection on mangrove development using  
2254  
2255 795 sediment cores and pollen analysis: A review. *Aquatic Botany* 89, 93–104.  
2256  
2257 796 Ellison, J.C., 2015. Vulnerability assessment of mangroves to climate change and  
2258  
2259 797 sea-level rise impacts. *Wetlands Ecology and Management*, 23(2), 115–137.  
2260  
2261 798 Engelhart, S.E., Horton, B.P., Roberts, D.H., Bryant, C.L., Corbett, D.R., 2007.  
2262  
2263 799 Mangrove pollen of Indonesia and its suitability as a sea level indicator. *Marine*  
2264  
2265 800 *Geology* 242, 65-81.  
2266  
2267 801 Fairbanks, R.G., 1989. A 17,000-year glacio-eustatic sea level record: influence of  
2268  
2269 802 glacial melting rates on the Younger Dryas event and deep- ocean circulation.  
2270  
2271 803 *Nature* 342, 639–642.  
2272  
2273  
2274  
2275  
2276  
2277  
2278  
2279  
2280

- 2281  
2282  
2283  
2284 804 Fisher, P. R., Dyer, K., Semesi, A. 1994. Rufiji Delta hydrodynamics research  
2285  
2286 805 program, Final report: Characteristic circulation and sedimentation in the Rufiji  
2287  
2288 806 delta, Tanzania. Frontier-Tanzania Technical report No. 13. The Society for  
2289  
2290 807 Environment Exploration. U.K.  
2291  
2292 808 Fleming, K., Johnston, P., Zwartz, D., Yokoyama, Y., Lambeck, K., Chappell, J.,  
2293  
2294 809 1998. Refining the eustatic sea-level curve since the Last Glacial Maximum using  
2295  
2296 810 far-and intermediate-field sites. *Earth and Planetary Science Letters* 163, 327–  
2297  
2298 811 342.  
2299  
2300 812 Francis, J. 1992. Physical processes in the Rufiji delta and their possible  
2301  
2302 813 implications on the mangrove ecosystem. *Hydrobiologia* 247, 173–179.  
2303  
2304 814 Gasse, F., 2000. Hydrological changes in the African tropics since the Last  
2305  
2306 815 Glacial Maximum. *Quaternary Science Reviews* 19, 189–211.  
2307  
2308 816 Gehrels, R., Long, A., 2008. Sea level is not level: the case for a new approach to  
2309  
2310 817 predicting UK sea-level rise. *Geography* 93(1), 11–16.  
2311  
2312 818 Gilman, E.L., Ellison, J., Duke, N.C. and Field, C., 2008. Threats to mangroves  
2313  
2314 819 from climate change and adaptation options: A review. *Aquatic Botany* 89(2),  
2315  
2316 820 237–250.  
2317  
2318 821 Goudie, A. S., 1996. Climate: past and present. In: Adams, W.A., Goudie, A.S.,  
2319  
2320 822 Orme, A.R. (eds) *The physical geography of Africa*. Oxford University Press,  
2321  
2322 823 New York, pp 34–59  
2323  
2324 824 Hait, A. K., Behling, H., 2009. Holocene mangrove and coastal environmental  
2325  
2326 825 changes in the western Ganga–Brahmaputra Delta, India. *Vegetation History and*  
2327  
2328 826 *Archaeobotany* 18, 159–169.  
2329  
2330 827 Hanebuth, T., Statterger, K., Grootes, P.M., 2000. Rapid Flooding of the Sunda  
2331  
2332 828 Shelf: A Late-Glacial Sea-Level Record. *Science* 288, 1033–1035.  
2333  
2334  
2335  
2336  
2337  
2338  
2339  
2340



2341  
2342  
2343  
2344  
2345  
2346  
2347  
2348  
2349  
2350  
2351  
2352  
2353  
2354  
2355  
2356  
2357  
2358  
2359  
2360  
2361  
2362  
2363  
2364  
2365  
2366  
2367  
2368  
2369  
2370  
2371  
2372  
2373  
2374  
2375  
2376  
2377  
2378  
2379  
2380  
2381  
2382  
2383  
2384  
2385  
2386  
2387  
2388  
2389  
2390  
2391  
2392  
2393  
2394  
2395  
2396  
2397  
2398  
2399  
2400

829 Hassan, F.A., 1997. Holocene Palaeoclimates of Africa. *African Archaeological*  
830 *Review* 14(4), 213–230.

831 Hijma, M., Engelhart, S.E., Törnqvist, T.E., Horton, B.P., Hu, P. and Hill, D.F.,  
832 2015. A protocol for a geological sea-level database. *Handbook of Sea-Level*  
833 *Research*, edited by: Shennan, I., Long, AJ, and Horton, BP, Wiley Blackwell, pp.  
834 536–553.

835 Horton, B.P., Benjamin, P., Gibbard, L.G., Milne, M., Morley, R.J.,  
836 Purintavaragul, C. and Stargardt, J.M., 2005. Holocene sea levels and  
837 palaeoenvironments, Malay-Thai Peninsula, Southeast Asia. *The Holocene* 15,  
838 1199–1213.

839 Isla, F.I., 1989. Holocene sea-level fluctuation in the Southern Hemisphere.  
840 *Quaternary Science Reviews* 8, 359–368.

841 Jaritz, W., Ruder, J., B, Schlenker, B., 1977. Das Quartar im Küstengebiet von  
842 Mocambique und seine Schwermineralführung. *Geologisches Jahrbuch, B*, 26: 3–  
843 93.

844 Katupotha, J., Fujiwara, K., 1988. Holocene sea level change on the southwest  
845 and south coasts of Sri Lanka. *Palaeogeography, Palaeoclimatology,*  
846 *Palaeoecology* 68, 189–203.

847 Kiage, L.M., Liu, K., 2006. Late Quaternary paleoenvironmental changes in East  
848 Africa: areview of multiproxy evidence from palynology, lake sediments, and  
849 associated records. *Progress in Physical Geography* 30 (5), 633–658.

850 Kibue, A. M., 2006. Sea level measurement and analysis in the Western Indian  
851 Ocean. National Report, Kenya.

852 Knopp, S., Mohammed, K.A., Simba Khamis, I., Mgeni, A.F., Stothard, J.R.,  
853 Rollinson, D., Marti, H., Utzinger, J., 2008. Spatial distribution of soil-transmitted

- 2401  
2402  
2403  
2404 854 helminths, including *Strongyloides stercoralis*, among children in Zanzibar.  
2405  
2406 855 Geospatial Health 3 (1), 47–56.  
2407  
2408 856 Lambeck, K., Nakada, M., 1990. Late Pleistocene and Holocene sea-level change  
2409  
2410 857 along the Australian coast. Palaeogeography, Palaeoclimatology, Palaeoecology  
2411  
2412 858 89, 143–176.  
2413  
2414 859 Lambeck, K., Rouby, H., Purcell, A., Sun, Y., Sambridge, M., 2014. Sea level and  
2415  
2416 860 global ice volumes from the Last Glacial Maximum to the Holocene. P Natl.  
2417  
2418 861 Acad. Sci. U. S. A. 111, 15296–15303.  
2419  
2420 862 Larcombe, P., Carter, R.M., Dye, J., Gagan, M.K., Johnson, D.P., 1995. New  
2421  
2422 863 evidence for episodic post-glacial sea-level rise, central Great Barrier Reef,  
2423  
2424 864 Australia. Marine Geology 127, 1–44.  
2425  
2426 865 Lewis, S.E., Sloss, C.R., Murray-Wallace, C.V., Woodroffe, C.D. and Smithers,  
2427  
2428 866 S.G., 2013. Post-glacial sea-level changes around the Australian margin: a review.  
2429  
2430 867 Quaternary Science Reviews, 74, pp. 115–138.  
2431  
2432 868 Machiwa, J.F., Hallberg, R.O., 1995. Flora and crabs in a mangrove forest partly  
2433  
2434 869 distorted by human activities. Zanzibar Ambio 24 (7–8), 492–496.  
2435  
2436 870 Mangora, M.M., Shalli, M.S., Semesi, I.S., Njana, M.A., Mwainunu, E.J., Otieno,  
2437  
2438 871 J.E., Ntibasubile, E., Mallya, H.C., Mukama, K., Wambura, M. and Chamuya,  
2439  
2440 872 N.A., 2016, January. Designing a mangrove research and demonstration forest in  
2441  
2442 873 the rufiji delta, Tanzania. In Proceedings of the 5th Interagency Conference on  
2443  
2444 874 Research in the Watersheds, pp. 190-192. US Department of Agriculture Forest  
2445  
2446 875 Service, Southern Research Station.  
2447  
2448 876 Marchant, R.A., Hooghiemstra, H., 2004. Rapid environmental change in Africa  
2449  
2450 877 and South American tropics around 4000 years before present. Earth Science  
2451  
2452 878 Reviews 66, 217–260.  
2453  
2454  
2455  
2456  
2457  
2458  
2459  
2460

- 2461  
2462  
2463  
2464 879 Masalu, D.C.P., 2003. Challenges of coastal area management in coastal  
2465  
2466 880 developing countries—lessons from the proposed Rufiji Delta prawn farming  
2467  
2468 881 project, Tanzania. *Ocean Coastal Management* 46, 175–188.  
2469  
2470 882 McCormac, F.G., Hogg, A.G., Blackwell, P.G., Buck, C.E., Higham, T.F.G.,  
2471  
2472 883 Reimer, P.J., 2004. SHCal04 Southern Hemisphere Calibration, 0–11.0 cal kyr  
2473  
2474 884 BP. *Radiocarbon* 46(3), 1087–1092.  
2475  
2476 885 McIvor, A.L., Spencer, T., Möller, I. and Spalding, M., 2013. The response of  
2477  
2478 886 mangrove soil surface elevation to sea level rise. *Natural Coastal Protection*  
2479  
2480  
2481 887 Series: Report 3. Cambridge Coastal Research Unit Working Paper 42. The  
2482  
2483 888 Nature Conservancy and Wetlands International. 59 pp.  
2484  
2485 889 Milne, G., Long, A., Bassett, S., 2005. Modelling Holocene relative sea-level  
2486  
2487 890 observations from the Caribbean and South America. *Quaternary Science*  
2488  
2489 891 *Reviews* 24, 1183–1202.  
2490  
2491 892 Milne, G.A., Mitrovica, J.X., 2008. Searching for eustasy in deglacial sea-level  
2492  
2493 893 histories. *Quaternary Science Reviews* 27, 2292–2302.  
2494  
2495 894 Mitrovica, J.X., Peltier, W.R., 1991. On postglacial geoid subsidence over the  
2496  
2497 895 equatorial oceans. *Journal of Geophysical Research* 96, 20053–20071.  
2498  
2499 896 Mitrovica, J.X., Milne, G.A., 2002. On the origin of late Holocene sea-level  
2500  
2501 897 highstands within equatorial ocean basins. *Quaternary Science Reviews* 21, 2179–  
2502  
2503 898 2190.  
2504  
2505 899 Mörner, N., 1992. Ocean circulation, sea level changes and east African coastal  
2506  
2507 900 settlements. In Sinclair, P.J.J., and Juma, A., (Eds.). *Urban Origins in Eastern*  
2508  
2509 901 *Africa: Proceedings of the 1991 Workshop in Zanzibar*. Stockholm: Swedish  
2510  
2511 902 Central Board of National Antiquities, pp. 256–266.  
2512  
2513  
2514  
2515  
2516  
2517  
2518  
2519  
2520

2521  
2522  
2523  
2524  
2525  
2526  
2527  
2528  
2529  
2530  
2531  
2532  
2533  
2534  
2535  
2536  
2537  
2538  
2539  
2540  
2541  
2542  
2543  
2544  
2545  
2546  
2547  
2548  
2549  
2550  
2551  
2552  
2553  
2554  
2555  
2556  
2557  
2558  
2559  
2560  
2561  
2562  
2563  
2564  
2565  
2566  
2567  
2568  
2569  
2570  
2571  
2572  
2573  
2574  
2575  
2576  
2577  
2578  
2579  
2580

903 Mörner, N.A., 1996. Global change and interaction of earth rotation, ocean  
904 circulation and paleoclimate. *Anais da Academia Brasileira de Ciências*, 68, 77-  
905 94.

906 Mwandya, A.W., Gullstrom, M., Andersson, M.H., Ohman, M.C., Mgya, Y.D.,  
907 Bryceson, I., 2010. Spatial and seasonal variations of fish assemblages in  
908 mangrove creek systems in Zanzibar (Tanzania). *Estuarine, Coastal and Shelf  
909 Science* 89(4), 277–286.

910 Nicholson, S.E., 2001. Climatic and environmental change in Africa during the  
911 last two centuries. *Climate research*, 17(2), 123-144.

912 Nshubemuki, L., 1993. Forestry resources in Tanzania’s wetlands: concepts and  
913 potentials. *Wetlands of Tanzania*, 37–48.

914 Norström, E., Risberg, J., Gröndahl, H., Holmgren, K., Snowball, I., Mugabe, J.A.  
915 Siteo, S.R., 2012. Coastal Paleo-environment and Sea-level Change at Macassa  
916 Bay, Southern Mozambique, Since c 6600 Cal BP. *Quaternary International* 260,  
917 153–163.

918 Oerlemans, J., 2001. *Glaciers and climate change*. Library of Congress  
919 Cataloging-in-Publication Data.

920 Pirazzoli, P. A., Montaggioni, L. F., Salvat, B., & Faure, G., 1988. Late Holocene  
921 sea level indicators from twelve atolls in the central and eastern Tuamotus (Pacific  
922 Ocean). *Coral Reefs*, 7(2), 57–68.

923 Pirazzoli, P.A., 1991: *World Atlas of Holocene sea level changes*. Elsevier,  
924 Amsterdam, 300 pp.

925 Prendergast, M.E., Rouby, H., Punnwong, P., Marchant, R., Crowther, A.,  
926 Kourampas, N., Shipton, C., Walsh, M., Lambeck, K. and Boivin, N.L., 2016.

- 2581  
2582  
2583  
2584 927 Continental island formation and the archaeology of defaunation on Zanzibar,  
2585  
2586 928 eastern Africa. PLoS ONE 11(2): e0149565.  
2587  
2588 929 Punwong, P., Marchant, R., Selby, K., 2012. Holocene mangrove dynamics and  
2589  
2590 930 environmental change in the Rufiji Delta, Tanzania. *Vegetation History and*  
2591  
2592 931 *Archaeobotany* 22(5), 381–396.  
2593  
2594 932 Punwong, P., Marchant, R., Selby, K., 2013a. Holocene mangrove dynamics from  
2595  
2596 933 Unguja Ukuu, Zanzibar. *Quaternary International* 298, 4–19.  
2597  
2598 934 Punwong, P., Marchant, R., Selby, K., 2013b. Holocene mangrove dynamics in  
2599  
2600 935 Makoba Bay, Zanzibar. *Palaeogeography Palaeoclimatology Palaeoecology* 379–  
2601  
2602 936 380, 54–67.  
2603  
2604 937 Ramsay, P.J, 1995. 9000 years of sea-level change along the southern African  
2605  
2606 938 coastline. *Quaternary International* 31, 71–75.  
2607  
2608 939 Ramsay, P.J., Cooper, J. A. G., 2002. Late Quaternary Sea-Level Change in South  
2609  
2610 940 Africa. *Quaternary Research* 57, 82–90.  
2611  
2612 941 Richmond, M. D., Wilson, J. D. K., Mgaya, Y. D., Le Vay, L. 2002. An analysis  
2613  
2614 942 of smallholder opportunities in fisheries, coastal and related enterprises in the  
2615  
2616 943 floodplain and delta areas of the Rufiji River, Tanzania. *Rufiji Environment*  
2617  
2618 944 *Management Project Technical report* (25), 89 pp.  
2619  
2620 945 Rijdsdijk, K.F., Zinke, J., de Loux, P.G.B., Hume, J.P., van der Plicht, H.,  
2621  
2622 946 Hooghiemstra, H., Meijer, H.J.M., Vonhof, H., Porch, N., Florens, V., Baider, C.,  
2623  
2624 947 van Geel, B., Brinkkemper, J., Vernimmen, T., Janoo, A., 2011. Mid-Holocene  
2625  
2626 948 (4200 kyr BP) mass mortalities in Mauritius (Mascarenes): Insular vertebrates  
2627  
2628 949 resilient to climatic extremes but vulnerable to human impact. *The Holocene*, 1–  
2629  
2630 950 16.  
2631  
2632  
2633  
2634  
2635  
2636  
2637  
2638  
2639  
2640

2641  
2642  
2643  
2644  
2645  
2646  
2647  
2648  
2649  
2650  
2651  
2652  
2653  
2654  
2655  
2656  
2657  
2658  
2659  
2660  
2661  
2662  
2663  
2664  
2665  
2666  
2667  
2668  
2669  
2670  
2671  
2672  
2673  
2674  
2675  
2676  
2677  
2678  
2679  
2680  
2681  
2682  
2683  
2684  
2685  
2686  
2687  
2688  
2689  
2690  
2691  
2692  
2693  
2694  
2695  
2696  
2697  
2698  
2699  
2700

951 Santisuk, T., 1983. Taxonomy and distribution of terrestrial trees and shrubs in  
952 the mangrove formations in Thailand. *The Natural History Bulletin of the Siam*  
953 *Society*. 5 (1), 63–91.

954 Schlüter, T., 1997. *Geology of East Africa*. Gebrüder Borntraeger, Berlin, 484 pp.

955 Semesi, A. K., 1992. The mangrove resource of the Rufiji delta, Tanzania. In:  
956 Matiza T, Chabwela HN (Eds.) *Wetlands conservation conference for southern*  
957 *Africa. Proceedings of the southern African development coordination conference*  
958 *held in Gaborono, Botswana, 3–5 June 1991*. Union Internationale pour la  
959 *Conservation de la Nature et de ses Ressources*, Switzerland (UICN), Gland, pp  
960 157–172.

961 Shennan, I., Innes, J. B., Long, A. J., & Zong, Y. 1995. Late Devensian and  
962 Holocene relative sea-level changes in northwestern Scotland: new data to test  
963 existing models. *Quaternary International*, 26, 97–123.

964 Shunula, J.P., 2002. Public awareness, key to mangrove management and  
965 conservation: the case of Zanzibar. *Trees* 16, 209–212.

966 Sloss, C. R., Murray-Wallace, C. V., & Jones, B. G., 2007. Holocene sea-level  
967 change on the southeast coast of Australia: a review. *The Holocene*, 17(7), 999–  
968 1014.

969 Stocker, T.F., Qin, D., Plattner, G.K., Tignor, M., Allen, S.K., Boschung, J.,  
970 Nauels, A., Xia, Y., Bex, B. and Midgley, B.M., 2013. IPCC, 2013: climate  
971 change 2013: the physical science basis. Contribution of working group I to the  
972 fifth assessment report of the intergovernmental panel on climate change.

973 Thompson, L.G., Mosley-Thompson, E., Davis, M.E., Henderson, K.A., Brecher,  
974 H.H., Zagorodnov, V.S., Mashiotta, T.A., Lin, P., Mikhaleiko, V.N., Hardy,

- 2701  
2702  
2703  
2704 975 D.R., Beer, J., 2002. Kilimanjaro ice core records: evidence of Holocene climate  
2705  
2706 976 change in tropical Africa. *Science* 298, 589–593.  
2707  
2708 977 Tossou, M.G., Akoègninoua, A., Balloucheb, A., Sowunmic, M.A., Akpagana,  
2709  
2710 978 K., 2008. The history of the mangrove vegetation in Bénin during the Holocene:  
2711  
2712 979 A palynological study. *Journal of African Earth Sciences* 52, 167–174.  
2713  
2714 980 Vedel, V., Behling, H., Cohen, M., Lara, R., 2006. Holocene mangrove dynamics  
2715  
2716 981 and sea-level changes in northern Brazil, inferences from the Taperebal core in  
2717  
2718 982 northeastern Pará State. *Vegetation History and Archaeobotany* 15, 115–123.  
2719  
2720 983 Verschuren, D., Laird, K.R. and Cumming, B.F., 2000. Rainfall and drought in  
2721  
2722 984 equatorial east Africa during the past 1,100 years. *Nature*, 403(6768), 410-414.  
2723  
2724 985 Watson, J. G. 1928. Mangrove forests of the Malay Peninsula. *Malayan Forest*  
2725  
2726 986 *Records* 6, 275 pp.  
2727  
2728 987 Woodroffe, C.D., Grindrod, J., 1991. Mangrove Biogeography: The Role of  
2729  
2730 988 Quaternary Environmental and Sea-Level Change. *Journal of Biogeography* 18,  
2731  
2732 989 479.  
2733  
2734 990 Woodroffe, S.A., Horton, BP, 2005. Holocene sea-level changes in the Indo-  
2735  
2736 991 Pacific. *Journal of Asian Earth Sciences* 25, 29–43.  
2737  
2738 992 Woodroffe, S.A., 2006. Holocene relative sea-level changes in Cleveland Bay,  
2739  
2740 993 North Queensland, Australia. PhD thesis, University of Durham, 155 pp.  
2741  
2742 994 Woodroffe, S. A., Long, A.J., Punwong, P., Selby, K., Bryant, C.L., Marchant, R.,  
2743  
2744 995 2015a. Radiocarbon dating of mangrove sediments to constrain Holocene sea-  
2745  
2746 996 level change on Zanzibar in the Southwest Indian Ocean. *The Holocene* 25(5),  
2747  
2748 997 820-831.  
2749  
2750  
2751  
2752  
2753  
2754  
2755  
2756  
2757  
2758  
2759  
2760

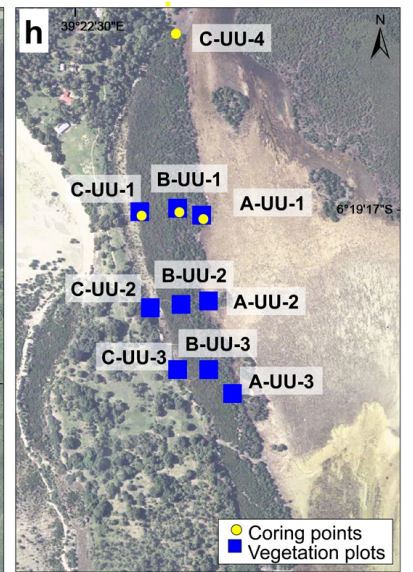
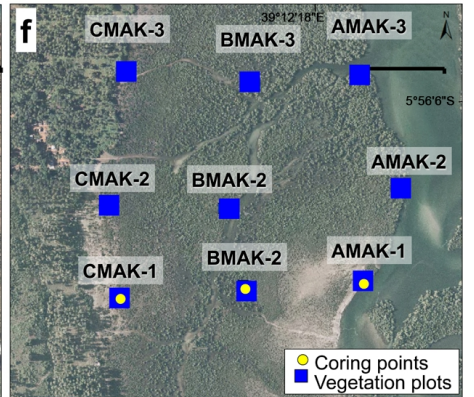
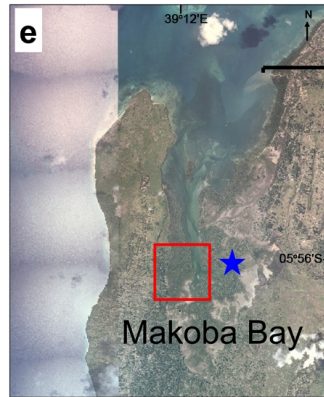
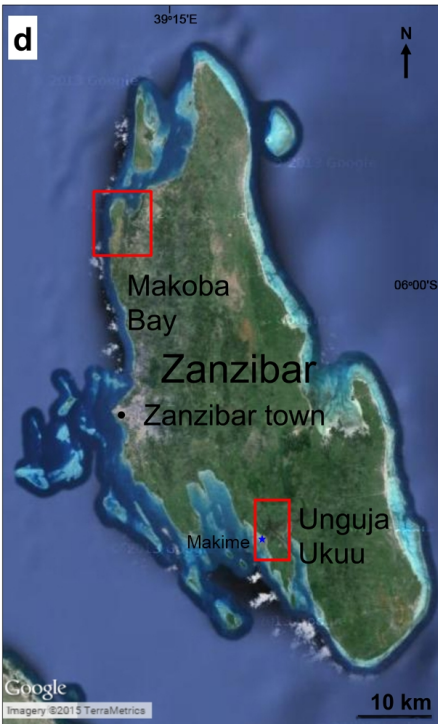
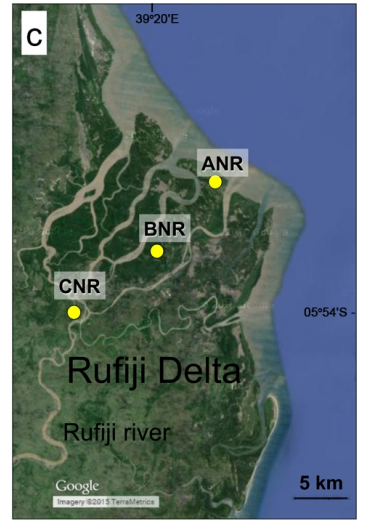
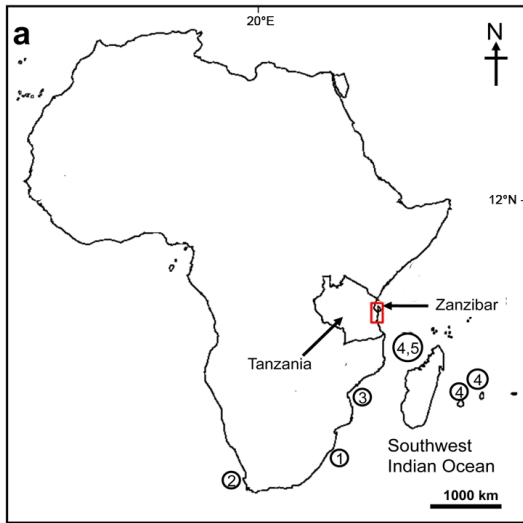
2761  
2762  
2763  
2764  
2765  
2766  
2767  
2768  
2769  
2770  
2771  
2772  
2773  
2774  
2775  
2776  
2777  
2778  
2779  
2780  
2781  
2782  
2783  
2784  
2785  
2786  
2787  
2788  
2789  
2790  
2791  
2792  
2793  
2794  
2795  
2796  
2797  
2798  
2799  
2800  
2801  
2802  
2803  
2804  
2805  
2806  
2807  
2808  
2809  
2810  
2811  
2812  
2813  
2814  
2815  
2816  
2817  
2818  
2819  
2820

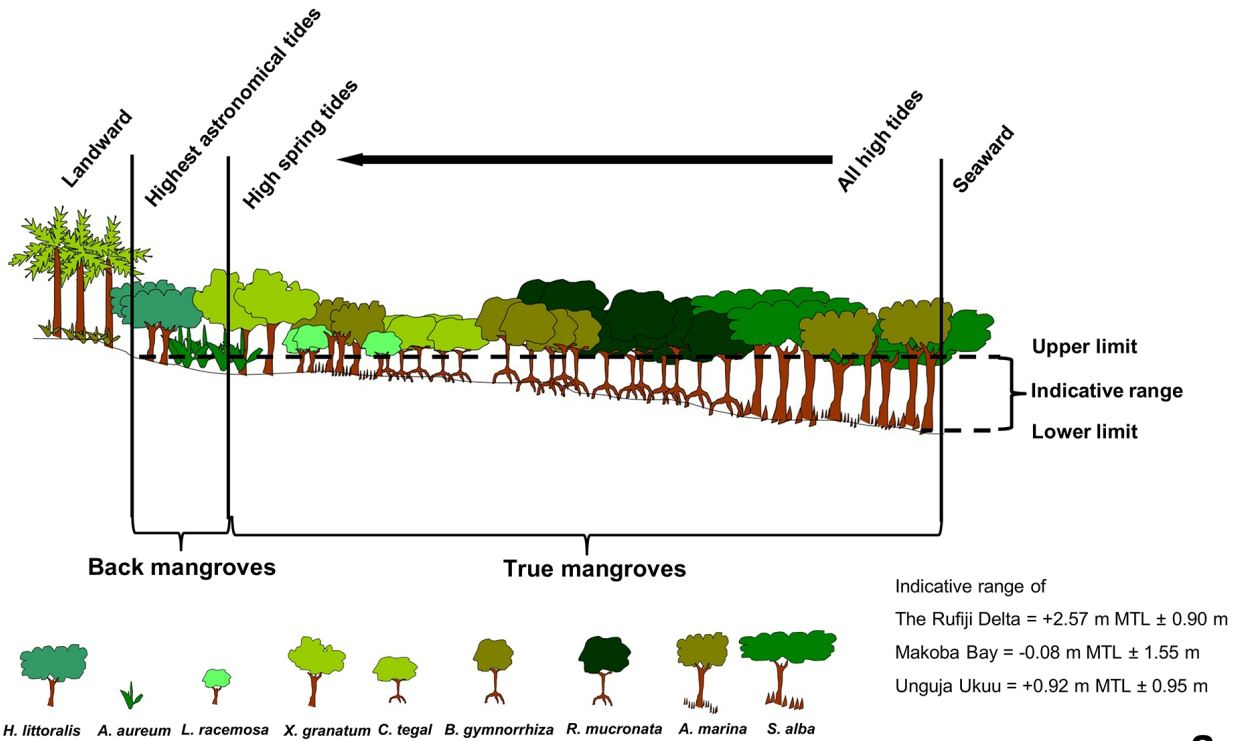
998 Woodroffe, S. A., Long, A. J., Milne, G. A., Bryant, C. L., & Thomas, A. L.  
999 2015b. New constraints on late Holocene eustatic sea-level changes from Mahé,  
1000 Seychelles. *Quaternary Science Reviews* 115, 1–16.

1001 Zinke, J., Reijmer, J.J.G., Dullo, W. C., Thomassin, B.A., 2000.  
1002 Paleoenvironmental changes in the lagoon of Mayotte associated with the  
1003 Holocene transgression. *Geolines* 11, 150–153.

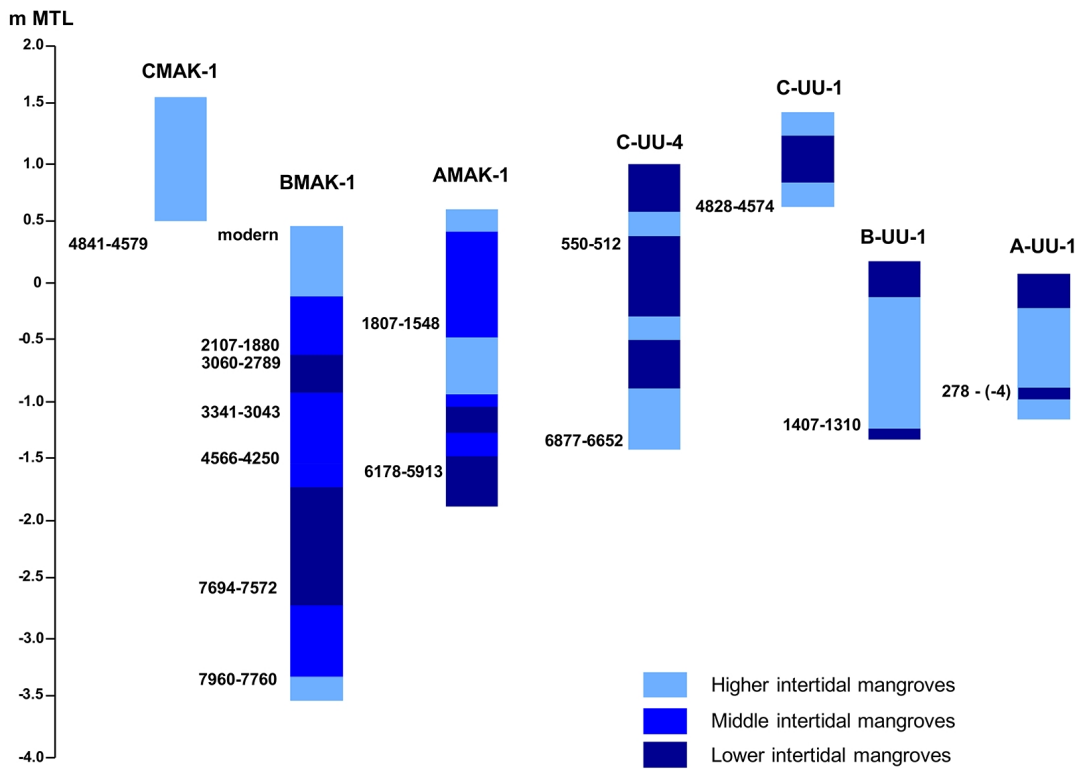
1004 Zinke, J., Reijmer, J.J.G., Thomassin, B.A., Dullo, W. C., Grootes, P.M. and  
1005 Erienkeuser, H., 2003. Postglacial flooding history of Mayotte Lagoon (Comoro  
1006 Archipelago, southwest Indian Ocean). *Marine Geology*, 194 (3-4), 181–196.



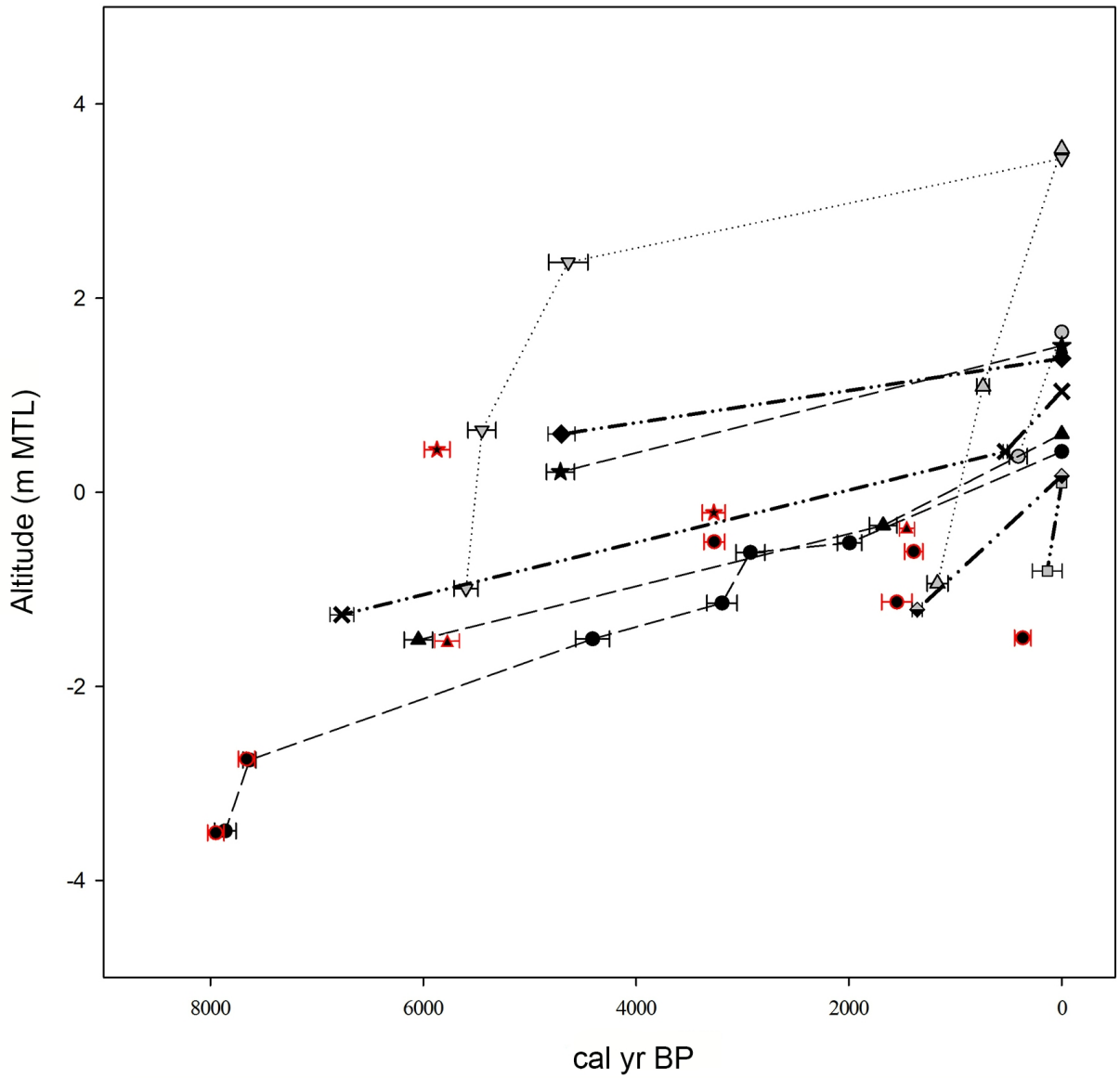




a



b



The Rufiji Delta

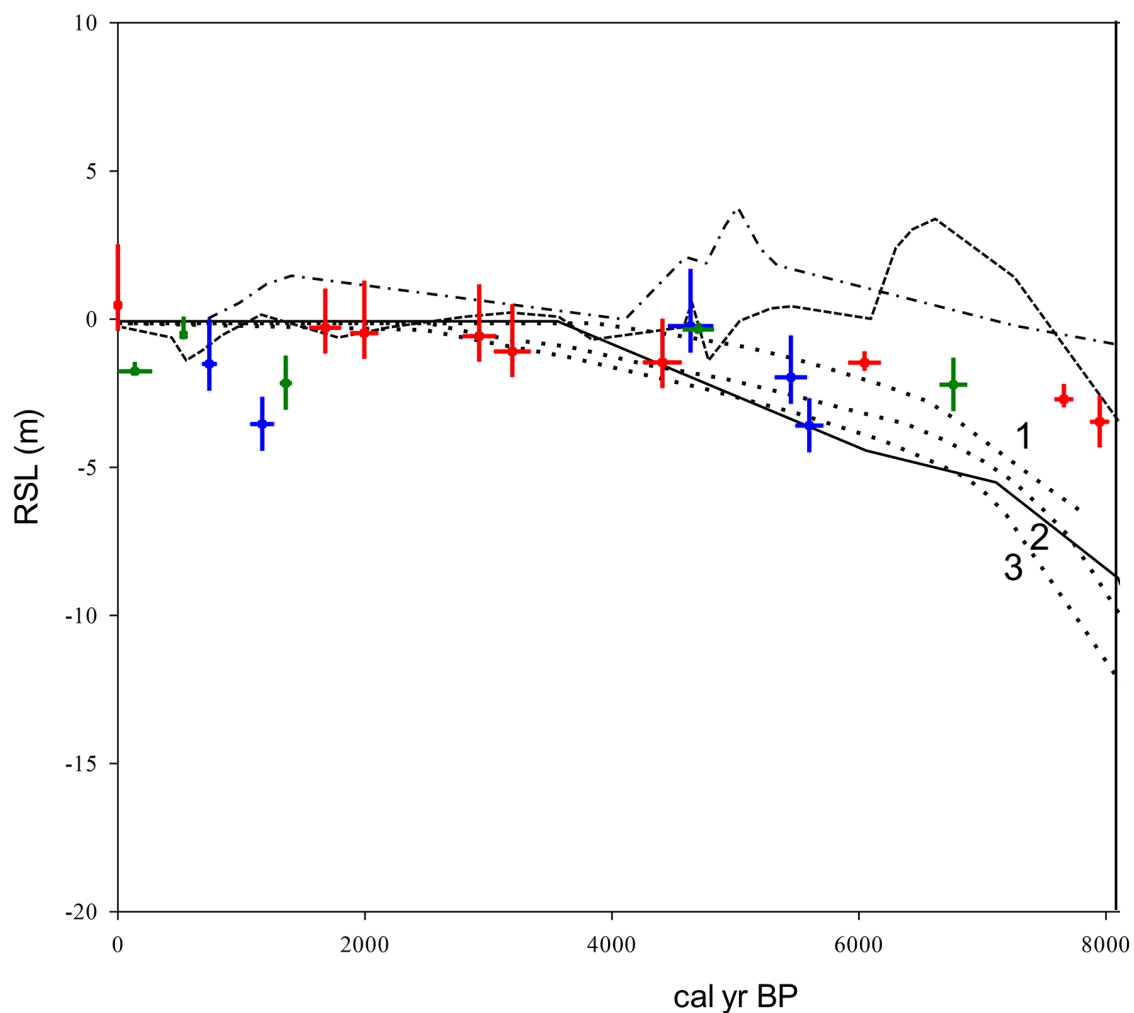
- .....○..... ANR
- .....▽..... BNR
- .....△..... CNR

Makoba Bay

- ▲--- AMAK-1
- BMAK-1
- ★--- CMAK-1

Unguja Ukuu

- A-UU-1
- ◇--- B-UU-1
- ◆--- C-UU-1
- ×--- C-UU-4



— RSL from The northern Rufiji Delta  
— RSL from Makoba Bay  
— RSL from Unguja Ukuu

- - - RSL from Compton (2001)  
 - . - RSL from Ramsay and Cooper (2002)  
 . . . RSL from Camoin et al. (1997; 2004)  
 (1) Mauritius, (2) Mayotte, (3) Réunion  
 — RSL from Zinke *et al.* (2003)